

การออกแบบหน่วยผลิตไฮโดรเจนสำหรับระบบเซลล์เชื้อเพลิงชนิดเมมเบรนแลกเปลี่ยนโปรตอนที่
ป้อนด้วยเมทานอล



นางสาวศิริพร บุญเครือ

ศูนย์วิทยทรัพยากร
จุฬาลงกรณ์มหาวิทยาลัย

วิทยานิพนธ์นี้เป็นส่วนหนึ่งของการศึกษาตามหลักสูตรปริญญาวิศวกรรมศาสตรมหาบัณฑิต


สาขาวิชาวิศวกรรมเคมี ภาควิชาวิศวกรรมเคมี

คณะวิศวกรรมศาสตร์ จุฬาลงกรณ์มหาวิทยาลัย

ปีการศึกษา 2552

ลิขสิทธิ์ของจุฬาลงกรณ์มหาวิทยาลัย

DESIGN OF HYDROGEN PROCESSOR FOR PROTON EXCHANGE MEMBRANE FUEL
CELL SYSTEM FUELLED BY METHANOL



Miss Siriporn Boonkrue

ศูนย์วิทยทรัพยากร
จุฬาลงกรณ์มหาวิทยาลัย
A Thesis Submitted in Partial Fulfillment of the Requirements
for the Degree of Master of Engineering Program in Chemical Engineering

Department of Chemical Engineering

Faculty of Engineering

Chulalongkorn University

Academic Year 2009

Copyright of Chulalongkorn University

ศิริพร บุญเครือ : การออกแบบหน่วยผลิตไฮโดรเจนสำหรับระบบเซลล์เชื้อเพลิงชนิดเมมเบรนแลกเปลี่ยนโปรตอนที่ป้อนด้วยเมทานอล. (DESIGN OF HYDROGEN PROCESSOR FOR PROTON EXCHANGE MEMBRANE FUEL CELL SYSTEM FUELLED BY METHANOL) อ. ที่ปรึกษาวิทยานิพนธ์หลัก: ศ.ดร.สุทธิชัย อัสสะบำรุงรัตน์, 80 หน้า.

ไฮโดรเจนนับเป็นเชื้อเพลิงที่ใช้อย่างแพร่หลายเข้าสู่เซลล์เชื้อเพลิงชนิดเมมเบรนแลกเปลี่ยนโปรตอนเพื่อผลิตไฟฟ้า อย่างไรก็ตามการใช้ไฮโดรเจนบริสุทธิ์ยังคงมีปัญหาในด้านการเก็บรักษาและการขนส่ง ดังนั้นจึงมีการพิจารณาถึงระบบผลิตไฮโดรเจนแบบติดตั้งด้วยกัมมันต์เมทานอลเป็นเชื้อเพลิง สำหรับกระบวนการรีฟอร์มมิ่งด้วยไอน้ำมีความน่าสนใจอย่างมาก เพราะสามารถผลิตไฮโดรเจนได้มากที่สุดเมื่อเปรียบเทียบกับกระบวนการรีฟอร์มมิ่งประเภทอื่นๆ แต่ผลิตภัณฑ์ที่ได้มันยังคงมีคาร์บอนมอนอกไซด์เหลืออยู่ ซึ่งจะเป็นพิษต่อเซลล์เชื้อเพลิงชนิดเมมเบรนแลกเปลี่ยนโปรตอน ดังนั้นต้องทำการลดปริมาณลง โดยใช้กระบวนการกำจัดคาร์บอนมอนอกไซด์ ในการศึกษาจะทำการเปรียบเทียบระหว่าง ระบบที่ 1 ซึ่งประกอบด้วยกระบวนการรีฟอร์มมิ่งด้วยไอน้ำและกระบวนการออกซิเดชันแบบเลือกเกิด และระบบที่ 2 ซึ่งประกอบด้วยกระบวนการรีฟอร์มมิ่งด้วยไอน้ำ, กระบวนการวอเตอร์แก๊สชิฟท์และกระบวนการออกซิเดชันแบบเลือกเกิด ในเทอมของขนาดของเครื่องปฏิกรณ์ ปริมาณไฮโดรเจนและความร้อนที่นำไปของระบบที่อุณหภูมิต่างๆ ของกระบวนการรีฟอร์มมิ่งด้วยไอน้ำ กระบวนการวอเตอร์แก๊สชิฟท์ (เฉพาะระบบที่ 2) และกระบวนการออกซิเดชันแบบเลือกเกิด เพื่อเลือกระบบที่เหมาะสมที่สุด ด้วยแบบจำลอง 1 มิติและมีอุณหภูมิคงที่

ระบบที่เหมาะสมที่สุดคือ ระบบที่ 1 ซึ่งสามารถผลิตไฮโดรเจนได้เพียงพอต่อการผลิตกระแสไฟฟ้าขนาด 50 กิโลวัตต์ในเซลล์เชื้อเพลิงชนิดเมมเบรนแลกเปลี่ยนโปรตอน โดยมีขนาด 29.20 กิโลกรัม สำหรับกระบวนการรีฟอร์มมิ่งด้วยไอน้ำและ 0.80 กิโลกรัม สำหรับกระบวนการออกซิเดชันแบบเลือกเกิด

ภาควิชา.....วิศวกรรมเคมี.....
สาขาวิชา.....วิศวกรรมเคมี.....
ปีการศึกษา.....2552.....

ลายมือชื่อนิสิต.....ศิริพร บุญเครือ.....
ลายมือชื่อ อ.ที่ปรึกษาวิทยานิพนธ์หลัก.....

5170629821 : MAJOR CHEMICAL ENGINEERING

KEYWORDS : STEAM REFORMING / METHANOL / HYDROGEN PRODUCTION /
FUEL CELL / MODELING

SIRIPORN BOONKRUE: DESIGN OF HYDROGEN PROCESSOR FOR
PROTON EXCHANGE MEMBRANE FUEL CELL SYSTEM FUELLED BY
METHANOL. THESIS ADVISOR: PROFESSOR SUTTICHA
ASSABUMRUNGRAT, Ph.D., 80 pp.

The hydrogen is a main fuel for proton exchange membrane fuel cell (PEMFC) for generating electricity. However, the usage of pure hydrogen in vehicle system confronts the problems related to hydrogen storage and transportation. Therefore, the on-board fuel processor is preferred and particularly when fuelled by methanol. For the reforming technology, the steam reforming was considered as the promising process as it offers highest hydrogen when compared with the others. However, the CO content in product should be reduced by CO clean-up systems before feeding to PEM fuel cell. In this work, the comparisons between SYS I consisting of steam reformer (SR) and preferential oxidation reactor (PROX) and SYS II consisting of SR, water gas shift reactor and PROX were investigated in terms of total catalyst weight, hydrogen production and energy consumption at various temperatures of steam reformer, WGS reactor (only for SYS II) and PROX reactor to select and design a suitable methanol-fuelled hydrogen production system for PEMFC. Mathematical model for all reactors as considered as isothermal and one-dimensional model.

SYS I is reported to be a suitable system for producing hydrogen for 50 kW PEMFC using 29.20 kg of steam reforming catalyst and and 0.80 kg of PROX reactor.

Department : ...Chemical Engineering.....

Student's Signature

Siriporn Boonkrue

Field of Study : ...Chemical Engineering.....

Advisor's Signature

Sutticha Assabumrungrat

Academic Year : ...2009.....

ACKNOWLEDGEMENTS

The author would like to express her sincere gratitude and appreciation to her advisor, Professor Dr. Suttichai Assabumrungrat, for their kindness, friendly, valuable suggestions, useful discussions and devotion to revise this thesis throughout the course of this Master Degree study. Furthermore, the author would also be grateful to Associate Professor Dr. Muenduen Phisalaphong, Associate Professor Dr. Anongnat Somwangthanaroj and Assistant Professor Dr. Worapon Kiatkittipong, for serving as chairman and member of thesis committees, respectively. The supports from the Thailand Research Fund and Commission on Higher Education and Graduate school of Chulalongkorn University is also gratefully acknowledged.

Most of all, the author would like to express her highest gratitude to her family who always pay attention to her all the times for suggestions, encouragement and financial support throughout this study. The most success of graduation is devoted to her family. Furthermore, I'd like to thanks Watcharapong Khawdee for knowledge support among her research.

Finally, the author wishes to thank the members and friends of the Center of Excellence on Catalysis and Catalytic Reaction Engineering, Department of Chemical Engineering, Faculty of Engineering, Chulalongkorn University who encouraged her and for their assistance over the years of her study.

ศูนย์วิจัยทรัพยากร
จุฬาลงกรณ์มหาวิทยาลัย

CONTENTS

	PAGE
ABSTRACT IN THAI.....	iv
ABSTRACT IN ENGLISH.....	v
ACKNOWLEDGEMENTS.....	vi
CONTENTS.....	vii
LIST OF TABLES.....	x
LIST OF FIGURES.....	xi
NOMENCLATURES.....	xv
CHAPTER	
I INTRODUCTION.....	1
II THEORY.....	3
2.1 Steam reforming process.....	3
2.1.1 Methanol steam reforming.....	4
2.1.2 Water-gas shift reaction.....	4
2.1.3 Preferential oxidation reaction.....	5
2.2 Fuel cells.....	5
2.2.1 Basic principles.....	5
2.2.2 Types of fuel cells.....	6
2.2.3 Fuel cell applications.....	6
2.3 Proton exchange membrane fuel cell (PEMFC).....	8
III LITERATURE REVIEWS.....	10
3.1 Hydrogen Production by Reforming Technology.....	10
3.2 Methanol Steam Reformer.....	13
3.3 CO Clean-Up Section.....	15
3.4 Integrated Methanol Reformer System.....	18
IV MATHEMATICAL MODELING.....	20

CHAPTER	PAGE
4.1 Mathematical models.....	20
4.2 Kinetic rate expression.....	20
4.2.1 Methanol steam reforming reaction.....	20
4.2.2 Water-gas shift reaction.....	22
4.2.3 Preferential oxidation reaction.....	22
4.3 Reactor modeling.....	22
4.3.1 Material balance.....	23
4.3.2 Simulation methods.....	23
V RESULTS AND DISCUSSION.....	25
5.1 Model validation.....	25
5.1.1 Methanol steam reformer.....	26
5.1.2 Water-gas shift reactor.....	27
5.1.3 Preferential oxidation reactor.....	28
5.2 Thermodynamic analysis for the different reactors.....	29
5.2.1 Methanol steam reformer.....	30
5.2.2 Water-gas shift reactor.....	33
5.3 Simulation results of SYS I.....	36
5.3.1 Steam reformer in SYS I.....	37
5.3.2 CO clean-up process in SYS I.....	42
5.4 Simulation results of SYS II.....	46
5.4.1 Steam reformer in SYS II.....	47
5.4.2 CO clean-up processes in SYS II.....	52
5.5 Comparison between SYS I and SYS II.....	66
VI CONCLUSIONS AND RECOMMENDATIONS.....	69
6.1 Conclusion.....	69
6.2 Recommendation.....	70
REFERENCES.....	71
APPENDICES.....	74

	PAGE
Appendix A.....	75
Appendix B.....	77
Appendix C.....	79
VITA.....	80



ศูนย์วิทยทรัพยากร
จุฬาลงกรณ์มหาวิทยาลัย

LIST OF TABLES

TABLE		PAGE
2.1	Mobile ions and operating temperatures for various fuel cells.....	7
4.1	The parameters for rate expression for steam reforming, decomposition and water-gas shift reaction (units are consistent with pressures in bar and overall rate in mol/kg _{cat} s) (Lattner and Harold, 2005 and Peppley et al., 1999).....	21
4.2	Operating conditions for SYS I	24
4.3	Operating conditions for SYS I	24
5.1	The mole fraction of component in feed stream to water-gas shift reactor.....	33
5.2	Mole fraction of components in outlet streams from the steam reformer SYS I.....	41
5.3	Heat requirement for operating steam reformer (SYS I).....	42
5.4	Mole fraction of components in outlet streams from the steam reformer SYS II.....	51
5.5	Heat requirement for operating steam reformer (SYS II).....	51
5.6	Mole fraction of components in outlet streams from the WGS reactor for SYS II at $X_{CO} = 0.003$	57
5.7	Mole fraction of components in outlet streams from the WGS reactor for SYS II at $X_{CO} = 0.004$	58
B.1	Gibb's free energy of formation (G_f) of components (kJ/mol).....	77
B.2	Heat capacities (C_p) of components (J/mol).....	78
B.3	Heat of formation (H_f) of components (kJ/mol).....	78

LIST OF FIGURES

FIGURE		PAGE
1.1	Schematic diagram of fuel processor and fuel cell system.....	2
2.1	Schematic diagram of a steam reforming process.....	3
2.2	A generic fuel cell schematic.....	6
5.1	Comparison the methanol conversion between literature (Pepply <i>et al.</i> , 1999) and our prediction model at S/M molar ratio = 1, temperature = 513, 533 K and $P = 1.01$ bar	26
5.2	Comparison of simulation results between literature (Choi and Stenger ,2003) and our prediction model for 1 kW fuel cell to achieve 1 mol% of exiting CO concentration.....	27
5.3	Comparison of the CO conversion between literature (Choi and Stenger, 2004) and our prediction model at various temperatures.....	29
5.4	Effect of temperature and S/M ratio on the equilibrium conversion of methanol in the steam reformer.....	30
5.5	Effect of temperature and S/M molar ratio on the hydrogen production in the steam reformer.....	31
5.6	Effect of temperature and S/M molar ratio on the equilibrium concentration of hydrogen in the steam reformer.....	32
5.7	Effect of temperature and S/M molar ratio on the equilibrium concentration of carbon monoxide in the steam reformer.....	32
5.8	Effect of S/C molar ratio and temperature on the equilibrium conversion of carbon monoxide in the water-gas shift reactor.....	34
5.9	Effect of temperature on the equilibrium conversion of carbon monoxide in the water-gas shift reactor at S/C molar ratio=2.0.....	34
5.10	Effect of temperature and S/C molar ratio on the equilibrium concentration of hydrogen in the water-gas shift reactor.....	35
5.11	Effect of temperature and S/C molar ratio on the equilibrium concentration of carbon monoxide in the water-gas shift reactor.....	35

FIGURE	PAGE
5.12 Schematic diagram of SYS I consisting of the steam reformer and the preferential oxidation reactor.....	36
5.13 Methanol conversion of steam reformer for SYS I.....	38
5.14 Hydrogen production rate of steam reformer for SYS I.....	38
5.15 CO concentration in product gas from steam reformer for SYS I.....	39
5.16 Catalyst weights for SR vs. temperature of SR at different methanol conversions for SYS I.....	39
5.17 Hydrogen production rate vs. temperature of SR at different methanol conversions for SYS I.....	40
5.18 Mole fraction of CO in SR outlet vs. temperature of SR at the different methanol conversions for SYS I.....	41
5.19 Catalyst weight of PROX reactor vs. temperature of PROX reactor at different conditions from the steam reformer ($[\text{CO}]_{\text{out}} = 50 \text{ ppm}$).....	43
5.20 Hydrogen production of PROX reactor vs. temperature of PROX reactor at the different conditions from the steam reformer ($[\text{CO}]_{\text{out}} = 50 \text{ ppm}$).....	43
5.21 Energy consumption for the PROX reactor.....	44
5.22 Total catalyst weight for SYS I vs. temperature of PROX reactor at different feed conditions from the steam reformer.....	45
5.23 Energy consumption for SYS I vs. temperature of PROX reactor and the steam reformer.....	46
5.24 Schematic diagram of SYS II consisting of the steam reformer, water-gas shift reactor and the preferential oxidation reactor.....	47
5.25 Methanol conversion of steam reformer for SYS II.....	48
5.26 Hydrogen production rate of steam reformer for SYS II.....	48
5.27 CO concentration in gas product of steam reformer for SYS II.....	49
5.28 Catalyst weights for SR vs. temperature of SR at different methanol conversions for SYS II.....	49

FIGURE	PAGE
5.29 Hydrogen productions in SR outlet vs. temperature of SR at different methanol conversions for SYS II.....	50
5.30 Mole fraction of CO in SR outlet vs. temperature of SR at different methanol conversions for SYS II.....	50
5.31 CO conversion vs. catalyst weight of WGS reactor at various temperatures of WGS reactor ($T_{SR} = 513\text{K}$).....	52
5.32 CO concentration vs. catalyst weight of WGS reactor at various temperatures of WGS reactor ($T_{SR} = 513\text{K}$).....	53
5.33 CO concentration vs. catalyst weight of WGS reactor at various temperatures of WGS reactor ($T_{SR} = 523\text{K}$).....	53
5.34 CO concentration vs. catalyst weight of WGS reactor at various temperatures of WGS reactor ($T_{SR} = 533\text{K}$).....	54
5.35 Catalyst weights of the WGS reactor vs. WGS temperatures at different reforming temperature feeds ($[\text{CO}]_{\text{out WGS}} = 0.003$).....	55
5.36 Catalyst weights of the WGS reactor vs. WGS temperatures at different reforming temperature feeds ($[\text{CO}]_{\text{out WGS}} = 0.004$).....	55
5.37 Hydrogen production rate for the WGS reactor at various temperatures of the WGS reactor for CO concentrations of 0.003 and 0.004.....	56
5.38 Energy consumption for the WGS reactor at $X_{\text{CO}} = 0.003$	58
5.39 Energy consumption for the WGS reactor at $X_{\text{CO}} = 0.004$	59
5.40 Catalyst weight of PROX reactor vs. T_{PROX} at X_{CO} inlet of 0.003 ($[\text{CO}]_{\text{out}} = 50\text{ ppm}$).....	60
5.41 Catalyst weight of PROX reactor vs. T_{PROX} at X_{CO} inlet of 0.004 ($[\text{CO}]_{\text{out}} = 50\text{ ppm}$).....	60
5.42 Hydrogen production rate of PROX reactor vs. temperature of PROX reactor at the different CO inlet concentrations ($[\text{CO}]_{\text{out}} = 50\text{ ppm}$).....	61
5.43 Energy consumption for the PROX reactor at X_{CO} inlet of 0.003.....	62
5.44 Energy consumption for the PROX reactor at X_{CO} inlet of 0.004.....	62

FIGURE	PAGE
5.45	Total catalyst weight for SYS II vs. T_{PROX} at the different conditions from the WGS reactor [$X_{\text{CO inlet PROX}} = 0.003$]..... 63
5.46	Total catalyst weight for SYS II vs. T_{PROX} at different conditions from the WGS reactor [$X_{\text{CO inlet PROX}} = 0.004$]..... 64
5.47	Energy consumption for SYS II vs. T_{PROX} at different conditions from the WGS reactor [$X_{\text{CO inlet PROX}} = 0.003$]..... 64
5.48	Energy consumption for SYS II vs. T_{PROX} at different conditions from the WGS reactor [$X_{\text{CO inlet PROX}} = 0.004$]..... 65
5.49	The comparison of hydrogen production between SYS I and SYS II.... 67
5.50	The comparison of total catalyst weight between SYS I and SYS II..... 68
5.51	The comparison of energy consumption between SYS I and SYS II..... 68



ศูนย์วิทยทรัพยากร
 จุฬาลงกรณ์มหาวิทยาลัย

NOMENCLATURES

C = Total surface concentration (mol/m^2)

F_i = Molar flow rate of species i (mol/s)

ΔH_j = Heat of reaction j (kJ/mol)

r_j = The rate constant of reactions j ($\text{mol}/\text{kg}_{\text{cat}} \text{ s}$)

K_j = The equilibrium constant of reactions j

K_i = The adsorption coefficient of species i

P = Pressure (bar)

p_i = Partial pressure of species i (bar)

R = The universal gas constant ($\text{J}/\text{mol K}$)

S_g = Surface area of catalyst (m^2/kg)

T = Temperature (K)

W = Mass of catalyst (kg)

GREEK LETTERS

κ = The additional parameter in equation of CO oxidation and H_2 oxidation.

v_{ij} = The stoichiometric coefficient for species i in reaction j

SUBSCRIPTS

$CH_3O^{(1)}$ = Adsorbed species CH_3O on active site S1

$CH_3O^{(2)}$ = Adsorbed species CH_3O on active site S2

CH_3OH = Methanol

CO = Carbon monoxide

CO = CO oxidation (eq. (4.7))

CO_2 = Carbon dioxide

D = Decomposition (eq. (4.3))

$H^{(1a)}$ = Adsorbed species H on active site S1a

$H^{(2a)}$ = Adsorbed species H on active site S2a

H_2 = Hydrogen

H_2 = H_2 oxidation (eq. (4.8))

H_2O = Steam

$HCOO^{(1)}$ = Adsorbed species $HCOO$ on active site S1

$HCOO^{(2)}$ = Adsorbed species HCOO on active site S2

N_2 = Nitrogen

O_2 = Oxygen

$OH^{(1)}$ = Adsorbed species OH on active site S1

$OH^{(2)}$ = Adsorbed species OH on active site S2

R = Direct reforming (eq. (4.1))

$S1, S1a, S2, S2a$ = Active site of the catalyst

W = Water-gas shift (eq. (4.2))

WGS = Water-gas shift reaction (eq. (4.5) and (4.9))

SUPERSCRIPTS

T = Total concentration of active sites

$*$ = Composite parameter

ACRONYM

PEMFC= Proton exchange membrane fuel cell

SR = Steam reformer

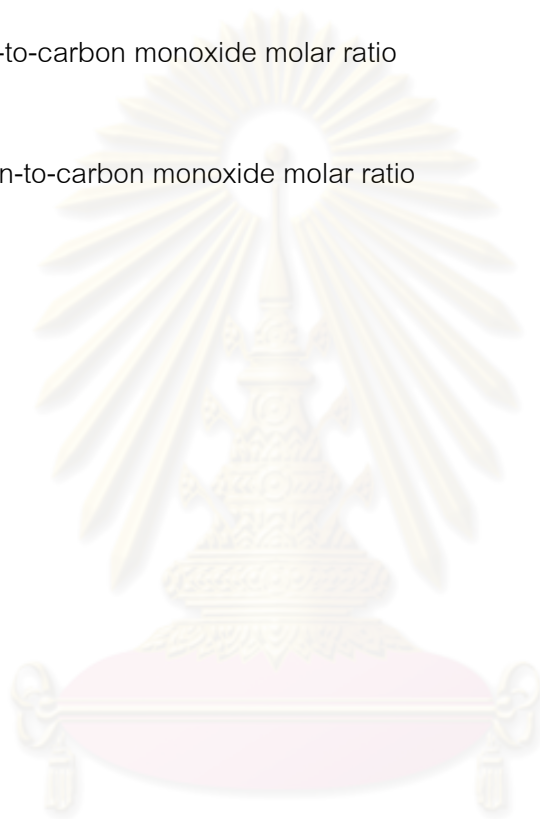
PROX = Preferential oxidation

WGS = Water-gas shift

S/M = Steam-to-methanol molar ratio

S/C = Steam-to-carbon monoxide molar ratio

O/C = Oxygen-to-carbon monoxide molar ratio



ศูนย์วิจัยทรัพยากร
จุฬาลงกรณ์มหาวิทยาลัย

CHAPTER I

INTRODUCTION

Fuels are very important for the public utilities especially in transportation section. Among several types of fuel, hydrogen is considered as a promising fuel for future applications. It can be used directly as an automotive fuel and as important reactant for production of other useful fuel. It is well known that fuel cell is one of the most attractive power generation systems that use hydrogen and oxygen as reactants and produce the clean energy as products. In details, fuel cell is an electrochemical device that converts the chemical energy of a fuel directly into electricity. Although, there are many types of fuel cell, proton exchange membrane fuel cell (PEMFC) is among the most interesting ones because PEMFC operates at low temperature with high efficiency and power density. Therefore, PEMFC is considered as a suitable type of fuel cell for automotive applications. However, the usage of pure hydrogen in vehicle system confronts the problems related to hydrogen storage and transportation. Therefore, the on-board fuel processor is preferred to liberate the hydrogen directly and methanol is often considered as a promising fuel source because it is stored as a liquid at atmosphere and can be reformed to hydrogen at relatively mild conditions (Lattner and Harold, 2005). Moreover, it has high hydrogen to carbon ratio.

The reforming technology for hydrogen production is currently based upon steam reforming, partial oxidation or autothermal reforming (Dudfield *et al.*, 2001). The steam reforming has an advantage of producing the highest hydrogen concentration when compared with partial oxidation and autothermal reforming, nevertheless, since this reaction is highly endothermic, it requires heat supply from external sources.

Typically, hydrogen produced from the steam reforming reaction always contains carbon monoxide, which easily poisons the anode of PEMFC. Hence, the hydrogen-rich gas produced from the steam reformer (SR) must be treated in order to

reduce carbon monoxide concentration to less than 50 ppm prior to feeding to PEMFC (Ouzounidou *et al.*, 2009). One method to reduce carbon monoxide is the application of preferential oxidation (PROX). However, water-gas shift (WGS) reactor is a preferred choice to be installed after the SR for reduction of CO concentration to 1% (Lattner and Harold, 2004). Thus, the efficiency of PROX reactor for CO removal as limitation to PEMFC is improved. Finally, the outlet stream from the WGS reactor is sent to the PROX reactor subsequently as shown in Figure 1.1.

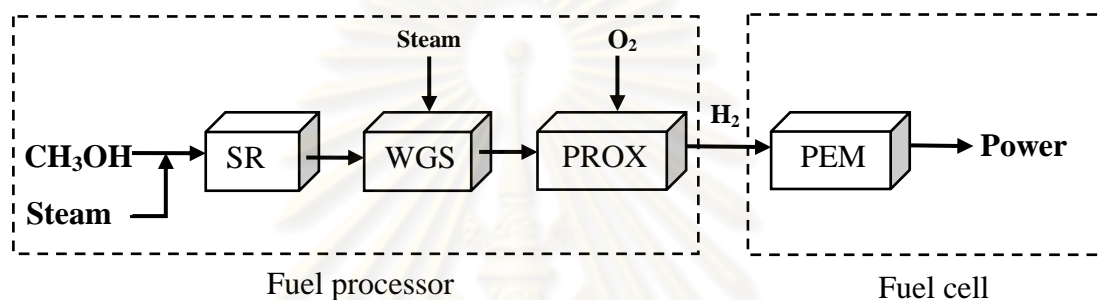


Figure 1.1. Schematic diagram of fuel processor and fuel cell system

In this work, mathematical models of SR, WGS reactor and PROX reactor are developed in MATLAB programs for simulating and designing the performance of different methanol-fuelled hydrogen systems for PEMFC whose CO concentration in the feed is limited at 50 ppm. Particular interest is focused on the comparison between the systems with and without WGS reactor. The sizes of the reactor, the hydrogen production rate and energy consumption are compared so that, a suitable system of hydrogen production for PEMFC can be selected.

The objective of this study is to compare and design a suitable methanol-fuelled hydrogen production system for PEMFC between two systems including i) SR and PROX reactor and ii) SR, WGS reactor and PROX reactor.

CHAPTER II

THEORY

2.1 Steam reforming process

Steam reforming is a technology for hydrogen production from hydrocarbons or alcohols. It is a strongly endothermic process that external heat is supplied to the reactor. The steam reforming reaction is reversible and the product stream is a mixture of hydrogen, carbon dioxide, carbon monoxide, water and some unreacted fuel. Figure 2.1 shows a schematic diagram of the steam reforming process for hydrogen production.

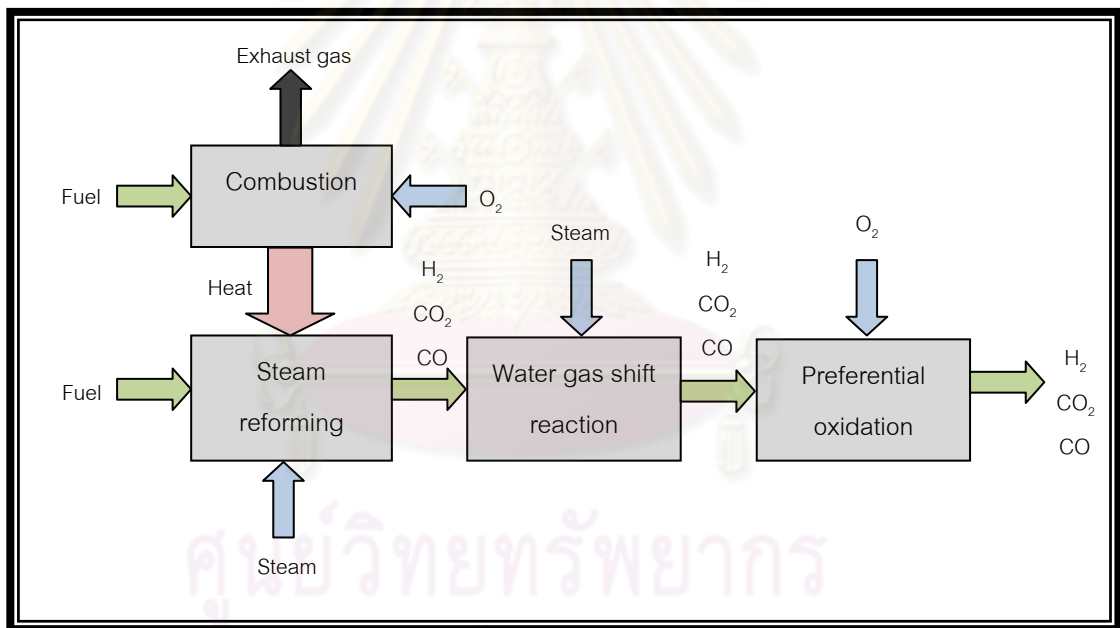
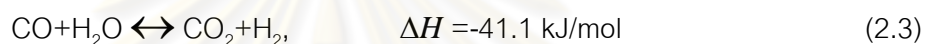
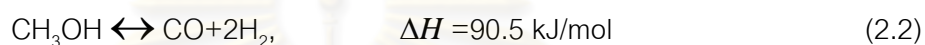
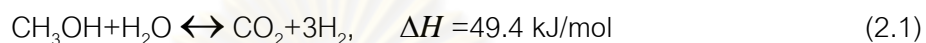


Figure 2.1 Schematic diagram of a steam reforming process.

The product stream from reformer still remains a significant amount of CO so that it is taken to the water gas shift reactor where CO reacts with steam and is converted to hydrogen and CO₂. However, the CO concentration in outlet stream still contains about 1% of CO, which would be harm to PEMFC. The CO content is further diminished in preferential oxidation process where CO is selectively oxidized with oxygen to produce CO₂.

2.1.1 Methanol steam reforming

The steam reforming of methanol is a familiar reaction with high efficiency. Generally, methanol and water are evaporated and react in a catalytic fixed bed reactor to carbon dioxide and hydrogen, the preferred product. The steam reforming reactions of methanol are as follows:



The three reactions that occur in the reformer include steam reforming, Eq. (2.1), methanol decomposition, Eq. (2.2), and water-gas shift, Eq. (2.3).

Steam reforming of methanol is observed as a possible way to provide fuel for fuel cell. The issue on hydrogen storage is still a main problem so, a methanol tank and steam reforming unit are used to solve this trouble. This might reduce the distribution problems related with hydrogen vehicles.

2.1.2 Water-gas shift reaction

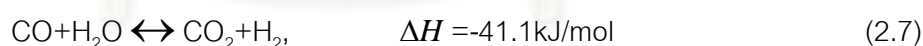
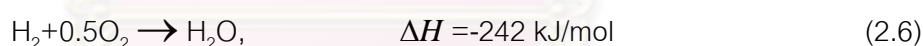
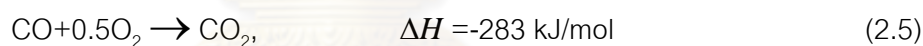
The water-gas shift reaction (WGS) is considered as secondary hydrogen maker and primary CO clean-up section. The carbon monoxide in the existence of steam is further converted to carbon dioxide and hydrogen. For the WGS step that benefits to reduce the volume of the subsequent CO removal step. The WGS is an exothermic reaction represented by the following equation below:



The process does not only reduce the amount of CO, but also raises the yield of H₂. WGS may compose a first clean-up step when the CO content is high, followed by secondary CO removal to reach part per million (ppm) levels. However, it is rather unlikely that the CO content in the WGS reactor can meet the low CO concentration specification for PEMFC feed.

2.1.3 Preferential oxidation reaction

The preferential oxidation is preferred to remove the CO from the reformat stream to ppm levels prior to use in the PEMFC. This will prevent CO poisoning of the PEMFC anode. In the preferential oxidation reactor, hydrogen-rich stream from steam reformer was mixed with oxygen and fed to PROX reactor to purify H₂ by eliminating CO. The reactions taken place in PROX reactor include CO oxidation, Eq. (2.5), H₂ oxidation, Eq. (2.6) and water-gas shift, Eq. (2.7).



2.2 Fuel cell

2.2.1 Basic principles

A fuel cell is an electrochemical device of power generation system that converts directly the chemical energy of fuel to electricity, usually hydrogen and oxidant, usually oxygen as shown in Figure 2.2. The fuel cell consists of two porous electrodes (anode and cathode), where the two electrochemical half reactions occur and separated by an electrolyte. The electrolyte in this fuel cell is an ion conduction polymer typically.

The major difference between galvanic cells and fuel cells is that fuel cells are considered as an energy conversion device while galvanic cells are considered as an energy storage device. Typical fuel cells are continuously fed by fuel/oxidant and operated until fuel/oxidant is no longer supplied to electrodes whereas galvanic cells use solution contained in the cell until the electrode is completely corroded.

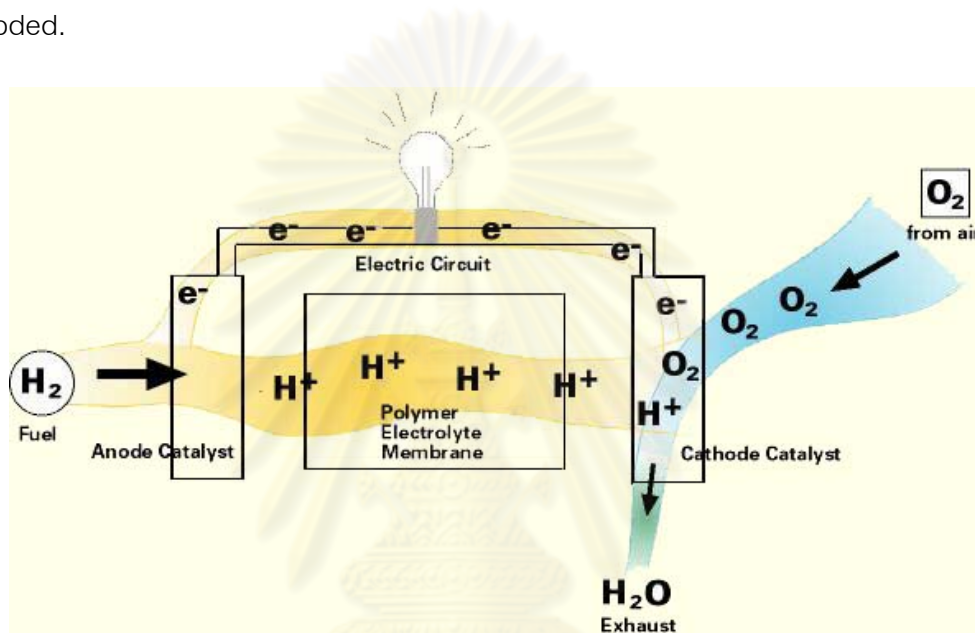


Figure 2.2 A generic fuel cell schematic.

2.2.2 Types of fuel cells

Types of fuel cell are typically classified by electrolyte materials which are extensively related to operating temperature. The information for each type of fuel cell is presented in Table 2.2.

Table 2.1 Mobile ions and operating temperatures for various fuel cells.

Fuel Cell Type	Mobile Ion	Operating Temperature
Alkaline (AFC)	OH^-	323-473 K
Proton exchange membrane (PEM)	H^+	323-373 K
Phosphoric acid (PAFC)	H^+	493 K
Molten carbonate (MCFC)	CO_3^{2-}	923 K
Solid oxide (SOFC)	O^{2-}	773-1273 K

2.2.3 Fuel cell applications

Due to different operating temperature and its power demand, their applications can be classified as follows.

2.2.3.1 Portable application

This type of fuel cell is used as a battery for a notebook or some electronic equipment due to its higher energy density.

2.2.3.2 Vehicle application

An important requirement for this application is quick start-up; therefore, low operating temperature is required. The fuel cell which is suitable for this propose is PEMFC. However, due to low operating temperature, the active electro-catalyst is necessary and the fuel introduced into the fuel cell must be purified.

2.2.3.3 Stationary application

High temperature fuel cells (i.e. SOFC and MCFC) are required for this application. Stationary application is generally for a power plant or auxiliary power for industrial or residential purpose.

2.3 Proton exchange membrane fuel cell (PEMFC)

Proton exchange membrane fuel cell (PEMFC) is a clean energy conversion device because the main products are only water, electricity and heat. The PEMFC has high efficiency, good dynamic behavior and also low operating temperature around 353 K.

At the anode side, hydrogen is supplied and oxidized, creating electrons and protons at the catalytic surface of anode. The electrons released in anode reaction (2.8) are transferred through an external circuit to the cathode side and H^+ ions migrated through the electrolyte to cathode also. At the cathode side, oxygen is supplied, when oxygen comes to catalytic surface of the cathode, it reacts with protons and electron to form water as cathode reaction (2.9). The reactions in a PEM fuel cell can be written as following:

The major difference between galvanic cells and fuel cells is that fuel cells are considered as an energy conversion device while galvanic cells are considered as an energy storage device. Typical fuel cells are continuously fed by fuel/oxidant and operated until fuel/oxidant is no longer supplied to electrodes whereas galvanic cells use solution contained in the cell until the electrode is completely corroded.





Water management in the membrane is a crucial factor for efficient performance. If water is not sufficient, the membrane becomes dehydrated and led to increasing the resistance of the proton conduction. In contrast, an excess of water can cause cell flooding, causing a problem on the oxygen diffusion in porous electrode.



ศูนย์วิทยทรัพยากร
จุฬาลงกรณ์มหาวิทยาลัย

CHAPTER III

LITERATURE REVIEWS

Proton exchange membrane fuel cell (PEMFC) is a promising technology for generating electricity. Its advantage is the low temperature operation that benefits for vehicle application. Generally, the fuels that supply to PEMFC are hydrogen and oxygen. Especially, hydrogen to be fed to PEMFC can be in pure hydrogen from a tank or hydrogen derived from an on-board fuel processor. However, the usage of pure hydrogen in vehicle system confronts the problems related to hydrogen storage and transportation. So, the on-board fuel processor is preferable to liberate the hydrogen directly. Normally, hydrogen can be produced by several reforming processes, i.e., steam reforming, partial oxidation and autothermal reforming process. However, the steam reforming process has attracted much research attention as it offers the highest hydrogen production. This chapter provides a review of the advance and development in steam reformer and CO clean-up system for hydrogen production to be used in PEMFC.

3.1 Hydrogen Production by Reforming Technology

Hydrogen is the reactant for use in fuel cells especially PEMFC to produce electricity which can be generated in fuel processor from the alternative fuels by means of the reforming reactions. Ahmed and Krumpelt (2001) studied the available fuel as $C_nH_mO_p$ with the different reforming reactions (steam reforming, partial oxidation and autothermal reforming). However, the efficiency of each reforming reaction was concerned with the fuel properties and the heat of formation of fuel that they virtually depended on the values of “m” and “n”. The results showed that the maximum efficiency in terms of a function of n, m and $\Delta H_{f, \text{fuel}}$ leads to increase with the H/C ratio (i.e., $m=n$). For reforming reactions, the steam reforming process offered the highest hydrogen production although it required the external heat sources.

Brown (2001) also studied the alternative fuels for hydrogen production including methanol, natural gas, gasoline, diesel fuel, aviation jet fuel, ethanol, and hydrogen. They compared the advantage and disadvantage of the different fuels to generate the hydrogen for PEMFC. The reactions used to create hydrogen consist of the reforming reactions (the steam reforming and the partial oxidation), water-gas shift reaction and preferential oxidation. The hydrogen produced by steam reforming contains ~70-80% while ~35-45% by partial oxidation. The lower fraction of hydrogen was the additional weakness using the partial oxidation. For comparison among different fuels, hydrogen is considered as the best fuel to generate the hydrogen for PEMFC. Nevertheless, it confronted with the severe storage and distribution problems. However, this work also studied the combination between steam reforming and partial oxidation of methanol as the rival fuel for on-board fuel processor.

Avcı et al. (2001) considered the conversion of the different fuels to hydrogen comprising of methane, propane, octane and methanol. In addition, the processes for hydrogen production were also studied between a direct partial oxidation and a combination of total oxidation and steam reforming. The results showed that the direct partial oxidation of propane and oxidation/steam reforming of octane are the best choices in terms of hydrogen production. However, they still faced with the CO formation problem.

Ersoz et al. (2006) studies the various reforming technologies i.e. steam reforming, partial oxidation and autothermal. In additional, they also compared the type of fuel that use to produce hydrogen as natural gas, gasoline and diesel by using Aspen-HYSYS 3.1 for evaluating the system efficiency. The operating condition was investigated at temperature between 973-1123 K, steam-to-carbon ratio 2.0-3.5 and pressure at 3 bar. The results showed that the highest fuel cell system efficiency was the steam reforming especially, fueled by natural gas was achieved at about 98% with heat integration at the S/C ratio of 3.5 and temperature around 1073 K. Anyway, the partial oxidation showed the lowest system efficiency.

Rabenstein and Hacker (2008) studied the thermodynamic analysis of hydrogen production from ethanol via the steam reforming, partial oxidation and combined autothermal reforming. The various processes were investigated in terms of steam-to-ethanol ratio (0.00–10.00), oxygen-to-ethanol ratio (0.00–2.50) and temperatures (473–1273 K) at atmospheric pressure. Thermodynamically favorable operating condition occurred at low temperature and the main product was methane which converted to hydrogen. Coke-formation preferred at low steam-to-ethanol ratios but the coke-formation free steam reforming was feasible over steam-to-ethanol ratio > 3. Finally, the results showed that the steam reforming achieved the highest system efficiency in terms of hydrogen production at high steam-to-ethanol ratio.

Lattner and Harold (2005) compared the different types of fuel processor fuelled by methanol such as steam reforming, autothermal reforming (ATR) and autothermal reforming (ATR) membrane reactor in terms of the overall system efficiencies and reactor volumes as a function of fuel processor design. They found that the efficiency of the ATR Pd membrane reactor was vaguely lower than the SR or ATR reactors. However, the main advantage of the ATR Pd membrane was a decrease of volume of fuel processor, at the expense of a more complex steam system and a small reduction

Kolavennu et al. (2006) designed the fuel cell power system for automotive applications. The systems composed of steam reformer, water-gas shift reactor, preferential oxidation and finally, fuel cell that can generate the electricity supplied to the automotive. The objective was to produce a combined model for the steady-state operation of a PEM fuel cell for automotive operation that fuelled by methane. The steam reformer was operated at 1000 K and 5.05 bar. The hydrogen production was found as 0.452 mol/s at methane conversion of 90%. The water-gas shift reactor was separated into two zones: a high temperature zone and a low temperature zone. For the PROX reactor, the oxygen-to-CO ration was kept at 2:1 and they found that the volume of $3.5 \times 10^{-4} \text{ m}^3$ was sufficient to reduce the CO concentration to 100 ppm.

For reforming processes, the steam reforming is seemed as the best fuel processor in term of high efficiency when compared with partial oxidation and auto-thermal reforming. However, the steam reforming showed the highest hydrogen production but it is an endothermic reaction so, heat supply is required. For using the natural gas as fuel to produce hydrogen still had problem with hydrogen storage and also, using ethanol that dealt with high operating temperature and methane occurred as main product at low temperature. Furthermore, the S/E ratio should be higher than 3 to avoid the coke formation so, the alternative fuel was investigated.

3.2 Methanol Steam Reformer

Methanol is often considered as a primary fuel source because it is stored as a liquid at atmosphere and can be reformed to hydrogen at relatively milder conditions than petroleum-based hydrocarbon. Moreover, it has high hydrogen to carbon ratio. Therefore, it seems to be an attractive fuel for on-board hydrogen production (Lattner and Harold, 2005).

The reactions involved in the production of hydrogen from methanol in a steam reformer can be summarized as follows:



Amphlett et al. (1994) studied the catalytic steam reforming from methanol to generate hydrogen for a PEMFC. Moreover, they developed a semi-empirical model over $\text{CuO}/\text{ZnO}/\text{Al}_2\text{O}_3$ catalyst. This analysis had quantified a number of factors which were relevant to design of reformer-fuel cell as the effect of temperature, pressure and steam-to-methanol ratio. They showed that the model can expect the

performance of the reformer with respect to the various parameters important in developing an integrated reformer-polymer fuel cell system.

Peppley et al. (1999) also studied a comprehensive model for the kinetics of methanol steam reforming on $\text{Cu/ZnO/Al}_2\text{O}_3$ catalyst. A set of Langmuir-Hinshelwood rate expression was derived based on a steady-state analysis of the final surface mechanisms. Finally, the results showed that the model was able to exactly predict the rate of hydrogen production, carbon dioxide and carbon monoxide for a wide range of operating conditions. They also confirmed the validity of kinetic models compared with the experimental data.

Lwin et al. (2000) investigated the thermodynamic equilibrium of steam reforming from methanol by varying mixtures of feed, temperatures (360-573 K) and steam-to-methanol molar ratio (0-1.5) via the minimization of Gibbs free energy. The results showed that the optimum condition for hydrogen production occurs at 1 atm pressure, 400 K and a steam-to-methanol ratio of 1.5 when the carbon and methane formations were not considered. At this condition, they found that the equilibrium concentration of CO is less than 1000 ppm and dimethyl ether (DME) is less than 300 ppm, with a hydrogen yield of 2.97 moles per mole of methanol and methanol conversion of 99.7%. Dimethyl ether formation occurred at low temperatures and low steam-to-carbon molar ratios whereas CO occurred at high temperatures and low steam-to-carbon molar ratio.

Mastalir et al. (2005) studied the kinetic model of steam reforming from methanol over $\text{Cu/ZrO}_2/\text{CeO}_2$ catalyst. The experiments were carried out under continuous operation in a fixed-bed reactor at atmospheric pressure, with steam-to-methanol ratio of 1:1. The raise of Cu content from 5 to 15% was found to improve the long-term stability and restrain the CO production considerably. Kinetic measurements were made in the temperature range of 503–573 K. They showed that the highest methanol conversions and the low CO levels were observed in the temperature range of 523–543 K.

Telotte et al. (2008) designed the steam reformer from methanol to produce sufficient hydrogen for generating a net power of 24 W and 72 W and they also used the rate expression of methanol steam reforming by Peppley *et al.* (1999). The reformer was modeled as a radial flow packed bed reactor and the Ergun equation was used to model the pressure drop. Effect of reactor temperature, inlet pressure and steam-to-methanol ratio were studied. They found that an inlet pressure of 202 kPa and a steam-to-methanol ratio of 1.5 were used to generate the sufficient hydrogen. The temperature 500 K was required for the lower power application as 550 K for the higher power application.

3.3 CO Clean-Up Section

The hydrogen-rich stream from steam reformer contained amount of carbon monoxide and if the mole fraction of carbon monoxide exceeds a certain level that will be poisoned to the electrode of PEM fuel cell. Therefore, removing carbon monoxide in a hydrogen-rich stream is a critical issue when hydrogen is used as the source of energy in such fuel cell types. One common method for reducing the carbon monoxide content of a hydrogen-rich stream while minimizing hydrogen conversion is preferential oxidation of carbon monoxide (PROX) (Vahabi and Akbari, 2009). Hydrogen-rich stream as fuel was mixed with oxygen and fed to PROX reactor to purify H₂ by eliminating CO. The reactions taken place in PROX reactor are as following:



Choi and Stenger (2004) studied the kinetics of CO preferential oxidation (PROX) on Pt-Fe/ γ -alumina catalyst to evaluate various rate expressions and to simulate

the performance the CO oxidation step of a methanol fuel processor for fuel cell applications. Temperature was varied between 373 and 573 K at atmospheric pressure. The effect of O₂/CO ratio, the effect of water addition, and various non-isothermal modes of operation were evaluated in these simulations. They showed that the trend of decreasing CO conversion and selectivity at higher temperatures is accurately predicted to be caused by the reverse water gas shift reaction rather than a difference in the activation energies for CO oxidation and H₂ oxidation. Also, it is shown that adding water should increase the performance of PROX reactor.

Dudfield et al. (2001) had designed, constructed and evaluated a compact CO preferential oxidation (PROX) reactor for PEM fuel cell applications as well as catalysts were studied to find a suitable catalyst for the particular reactor application i.e. acceptable CO oxidation activity and selectivity within a temperature range of 403–473 K. The reactor design was based upon the catalyst coating of high surface area heat transfer technology. They found that the PROX reactor can be successfully integrated and commissioned with a methanol steam reformer with reductions in fuel CO concentrations of 2.7% to < 20 ppm being subsequently demonstrated.

Francesconi et al. (2007) designed the water-gas shift (WGS) reactor to reduce the CO content from the outlet stream from ethanol fuel processor. They investigated a model-based reactor optimization to obtain both designs for reducing volumes and optimal operating conditions. The volume of WGS reactor is the largest component because the WGS reaction is very slow when compared with the other reactions that concerned in the reforming process and due to its inhibition of the thermodynamic equilibrium at high temperature. The results showed that the heterogeneous model used allows computing the optimal reactor length and diameter and the optimal catalyst particle diameter. Several reactors configurations are analyzed in order to state the limiting values of the main design variables. Specially, insulation conditions are studied in detail to access minimum total volumes.

Oliva et al. (2008) investigated the CO-PROX reactor design by model-based optimization. They added the different reactor components to show how the system dimensions and configuration changed after optimization. The rate expression of PROX reaction was preferred to use from Choi and Stenger (2004) and they developed this expression to avoid the numerical problems and to facilitate convergence. The heterogeneous reactor model was used to compute the optimal reactor length and diameter, optimal catalyst particle diameter, optimal insulating material thickness, as well as the optimal inlet temperature of the stream to operate the system in a pseudo-adiabatic mode.

Vahabi and Akbari (2009) investigated the three-dimensional numerical simulations of the reacting flow in rectangular microchannel PROX reactors. They proposed that the kinetics chosen were for a Pt-Fe/ γ -Al₂O₃ catalyst and operating temperatures of about 373 K and also the effects of the inlet steam content, oxygen to carbon monoxide ratio, reactor wall temperature, aspect ratio of the channel cross section, and the channel hydraulic diameter were investigated. The results showed that the optimum design conditions are as follows: steam content of 0.96×10^{-8} m³/s and oxygen-to-carbon monoxide ratio of 3 at the inlet, wall temperature of 393 K, a micro-channel with 300 mm hydraulic diameters and square cross-section. Such a PROX micro-reactor could deplete 2.3% carbon monoxide at the inlet to 7 ppm at the outlet in a 2.64mm length.

However, using PROX reactor following the steam reformer directly has strictly effect on the sizing of PROX reactor so, the water-gas shift (WGS) reactor is proposed to deal with this trouble. The water gas shift reaction is a critically significant reaction to shift carbon monoxide and water to hydrogen and carbon dioxide before feeding to PROX reactor.

3.4 Integrated Methanol Reformer System

An integrated methanol reformer system was combined commonly with steam reformer and CO clean-up section (PROX reactor and/or WGS reactor) to provide relatively pure hydrogen to a fuel cell.

Choi and Stenger (2005) evaluated reaction rates for making hydrogen from methanol via three reactors as the steam reformer, WGS reactor and PROX reactor. In this work, Cu-ZnO/Al₂O₃ catalyst was used for the steam reformer and WGS reactor and Pt-Fe/ γ -alumina catalyst was proposed for PROX reactor. The activity tests were performed between 393 and 598 K at atmospheric pressure with a range of feed rates and compositions. The product distribution, the effects of reactor volume and temperature, and the options of water and air injection rates were studied. The result showed that the performance of the integrated system was greatly affected by the size of the reformer and not sensitive to the temperature of the WGS reactor or PROX reactor. For best performance, the WGS reactor should be operated in the range of 493 K regardless of other process conditions. For PROX reactor, the operating temperature and reactor size had less impact on the performance of the reactor, but O₂/CO ratio should be maintained at a value higher than stoichiometry to avoid high CO concentrations in the final product.

Kamarudin et al. (2004) proposed a conceptual design of a fuel processor system for a 5 kW proton electrolyte membrane fuel cell (PEMFC) system for mobile and portable applications. The first section described the auto-thermal reformer (ATR) system while the second section demonstrated the significance of the water gas shift (WGS) reaction in the system. The main target was to produce the concentration of CO at less than 2000 ppm before entering the separation units. They found that if the mole ratio of O₂/C is 0.20–0.25, then the hydrogen selectivity is around 2.5–2.6 for complete methanol. Steam was fed at excess condition in both units, ATR and WGS, to avoid reverse WGS reaction. The conceptual design also proved the significance of WGS reaction in the reduction of CO produced in the ATR and indicated the importance

of pressure to reduce the bulk size of WGS reactor. The CO level was then further reduced to less than 2000 ppm after the WGS reactor. In addition, this paper also studied the performance of preferential oxidation (PROX) in removing the CO and it was observed that the PROX could reduce the CO to less than 100 ppm and performed better than WGS reaction in terms of water management.

Francesconi et al. (2007) investigated the energy integration and determined the maximum efficiency of an ethanol processor for hydrogen production and fuel cell operation. The fuel processor was comprised of steam reforming, followed by high- and low-temperature shift reactors and preferential oxidation, which were coupled to a PEM fuel cell. The heat exchanger network was implemented using the HYSYS program, which allowed analyzing the system energy integration by the process integration method. They found that a net electric efficiency around 35% was calculated based on the ethanol HHV. An efficient ethanol processor depended on the operating conditions of the reformer and their efficient energetic integration. This preliminary analysis was used to design the HEN system and perform a more accurate optimization in order to synthesize the process network.

Ratnamala et al. (2005) also studied the energy integration in a fuel processor, i.e., desulfurizer, steam reformer, high-temperature shift reactor, low-temperature shift reactor, preferential oxidation reactor, and various heat exchangers by using liquefied petroleum gas (LPG) as the fuel. The results obtained from the studies showed that the steam reforming with LPG gives a higher concentration of hydrogen in the product of about 74%. The fuel cell efficiency is around 34%, and the thermal efficiency including lean gas is about 93%. Furthermore, this model developed can serve as the basis for the development of an integrated PEMFC decentralized power pack for household applications.

CHAPTER IV

MATHEMATICAL MODELLING

4.1 Mathematical models

The hydrogen supplying to PEMFC can be generated by a series of fuel processors. In this study, the processor includes combined units of a steam reformer and CO clean-up system fuelled by methanol. Therefore, the mathematical models of each of reactor are provided. Besides, the rate expressions for the relevant reactions are provided as necessary for the mathematical modelling.

4.2 Kinetic rate expressions

4.2.1 Methanol steam reforming reaction

The kinetic rate expressions for the methanol steam reforming based on Cu/ZnO/Al₂O₃ catalysts are given by Peppley et al. (1999) as shown in the following expressions: Eqs. (4.1) - (4.3).

$$r_R = \frac{k_R K_{CH_3O^{(1)}}^* (p_{CH_3OH} / p_{H_2}^{1/2}) (1 - p_{H_2}^3 p_{CO_2} / K_R p_{CH_3OH} p_{H_2O}) C_{S1}^T C_{S1a}^T S_g}{(1 + K_{CH_3O^{(1)}}^* (p_{CH_3OH} / p_{H_2}^{1/2}) + K_{HCOO^{(1)}}^* p_{CO_2} p_{H_2}^{1/2} + K_{OH^{(1)}}^* (p_{H_2O} / p_{H_2}^{1/2})) (1 + K_{H^{(1a)}}^{1/2} p_{H_2}^{1/2})} \quad (4.1)$$

$$r_D = \frac{k_D K_{CH_3O^{(2)}}^* (p_{CH_3OH} / p_{H_2}^{1/2}) (1 - p_{H_2}^2 p_{CO} / K_D p_{CH_3OH}) C_{S2}^T C_{S2a}^T S_g}{(1 + K_{CH_3O^{(2)}}^* (p_{CH_3OH} / p_{H_2}^{1/2}) + K_{OH^{(2)}}^* (p_{H_2O} / p_{H_2}^{1/2})) (1 + K_{H^{(2a)}}^{1/2} p_{H_2}^{1/2})} \quad (4.2)$$

$$r_W = \frac{k_W K_{OH^{(1)}}^* (p_{CO} p_{H_2O} / p_{H_2}^{1/2}) (1 - p_{H_2} p_{CO_2} / K_W p_{CO} p_{H_2O}) C_{S1}^T S_g}{(1 + K_{CH_3O^{(1)}}^* (p_{CH_3OH} / p_{H_2}^{1/2}) + K_{HCOO^{(1)}}^* p_{CO_2} p_{H_2}^{1/2} + K_{OH^{(1)}}^* (p_{H_2O} / p_{H_2}^{1/2}))^2} \quad (4.3)$$

The three reactions that take place in the steam reformer include steam reforming, Eq. (4.1), methanol decomposition, Eq. (4.2), and water-gas shift, Eq. (4.3). The parameters of reaction rate constant applied for the calculations of the reaction rate are summarized in Table 4.1.

Table 4.1 the parameters for rate expression for steam reforming, decomposition and water-gas shift reaction (units are consistent with pressures in bar and overall rate in mol/kg_{cat} s) (Lattner and Harold, 2005 and Peppley et al., 1999).

Parameter	Expression
$C_{s1} = C_{s2}$ (mol m ⁻²)	7.5×10^{-6}
$C_{s1a} = C_{s2a}$ (mol m ⁻²)	1.5×10^{-5}
k_R (m ² s ⁻¹ mol ⁻¹)	$7.4 \times 10^{14} \exp(-102800/RT)$
k_D (m ² s ⁻¹ mol ⁻¹)	$3.8 \times 10^{20} \exp(-170000/RT)$
k_W (m ² s ⁻¹ mol ⁻¹)	$5.9 \times 10^{13} \exp(-87600/RT)$
$K_{CH_3O}^*$ ⁽¹⁾	$6.55 \times 10^{-3} \exp(20000/RT)$
$K_{CH_3O}^*$ ⁽²⁾	$36.9 \exp(20000/RT)$
K_{OH}^* ⁽¹⁾	$4.74 \times 10^{-3} \exp(20000/RT)$
K_{OH}^* ⁽²⁾	$36.9 \exp(20000/RT)$
$K_{H^{(1a)}}$	$5.43 \times 10^{-6} \exp(50000/RT)$
$K_{H^{(2a)}}$	$3.86 \times 10^{-3} \exp(50000/RT)$
K_{HCOO}^* ⁽¹⁾	$2.30 \times 10^9 \exp(-100000/RT)$

For the reaction equilibrium constant for reaction j can be calculated as follows:

$$K_j = \exp\left(\frac{-\Delta G_j}{RT}\right) \quad (4.4)$$

4.2.2 Water-gas shift reaction

For the water gas shift reaction, the rate expressions for WGS reactor are based on Cu/Zn/Al₂O₃ catalyst (Choi and Stenger, 2003) as shown in Eq. (4.5).

$$r_{WGS} = 8.01 \times 10^4 \exp\left(\frac{-47400}{RT}\right) \left(P_{CO} P_{H_2O} - \frac{P_{CO_2} P_{H_2}}{K_{WGS}} \right) \quad (4.5)$$

$$\text{Where } K_{WGS} = \exp\left(\frac{4577.8}{T} - 4.33\right) \quad (4.6)$$

4.2.3 Preferential oxidation reaction

For the preferential oxidation, the rate expressions for PROX reactor are based on Pt-Fe/ γ -Al₂O₃ catalyst by Choi and Stenger (2004) and after that, Oliva *et al.* (2008) modified the original expressions in order to avoid the numerical problems using the additional parameter \mathbf{K} equal to 1×10^{-6} in equation of CO oxidation and H₂ oxidation. The kinetic expressions were shown as below:

$$r_{CO} = 97.4854 \exp\left(\frac{-33092}{RT}\right) \left((P_{O_2} + \kappa)^{0.5} - \kappa^{0.5} \right) \left(\frac{P_{CO}}{\kappa + P_{CO}^{1.1}} \right) \quad (4.7)$$

$$r_{H_2} = 5.6656 \exp\left(\frac{-18742}{RT}\right) \left((P_{O_2} + \kappa)^{0.5} - \kappa^{0.5} \right) \quad (4.8)$$

$$r_{WGS,P} = 1.1910 \times 10^3 \exp\left(\frac{-34104}{RT}\right) \left(P_{CO} P_{H_2O} - \frac{P_{CO_2} P_{H_2O}}{K_{WGS}} \right) \quad (4.9)$$

Where K_{WGS} is given in Eq. (4.6).

4.3 Reactor modeling

All the reactors are modeled as plug flow reactors and based on the following basic assumptions:

- (1) One-dimensional mathematical model.
- (2) Isothermal condition for all reactors.
- (3) Operating at isobaric condition.
- (4) Ideal gas behavior.
- (5) The pressure drop inside reactors is negligible.
- (6) There is no axial mixing.

4.3.1 Material balance

With the assumptions specified above, the molar balance equations for component i can be integrated along with the weight of catalyst as below.

$$\frac{dF_i}{dW} = \sum_j \nu_{ij} r_j \quad (4.1)$$

Where the subscript i refers to the species i and j refers to the reaction j .

The stoichiometric coefficient for component i in reaction j is represented by ν_{ij} .

4.3.2 Simulation methods

The sizing of fuel processor from methanol was calculated approximately using the kinetic expressions integrated with one-dimensional components as shown as Eq. (4.1). The target of hydrogen production is designed for 50 kW PEM fuel cell that hydrogen required 0.5 mol/s (Kolavennu *et al.*, 2006). The flow rate of methanol was set at 0.18 mol/s. All of the simulations in this study were carried out with the MATLAB software using the stiff ordinary differential equations routine ode15s.

Table 4.2 Operating conditions for SYS I.

Reactors	Temperature (K)	S/M ratio	O/C ratio	Pressure (bar)
Steam reformer	433-533	2.0	-	1.01325
PROX reactor	423-523	-	2.0	1.01325

Table 4.3 Operating conditions for SYS II.

Reactors	Temperature (K)	S/M ratio	O/C ratio	Pressure (bar)
Steam reformer	433-533	1.5	-	1.01325
WGS reactor	393-513	-	-	1.01325
PROX reactor	423-523	-	2.0	1.01325

For operating conditions of SYS I and SYS II are summarized in Tables 4.2 and 4.3, respectively. However, the steam needs to provide instantly for the WGS reactor in SYS II. For the comparison between SYS I and SYS II, the steam supply should be equivalent mutually.

CHAPTER V

RESULTS AND DISCUSSION

Two hydrogen production systems from methanol are considered in this study. The first system (SYS I) is a combined steam reformer and preferential oxidation reactor and the other (SYS II) is a combined steam reformer, water-gas shift reactor and preferential oxidation reactor. The methanol steam reformer is packed with Cu/ZnO/Al₂O₃ catalysts (Pepply *et al.*, 1999) and the same catalyst is also used in water-gas shift reactor (Choi and Stenger, 2003). For preferential oxidation reactor, Pt-Fe/ γ -alumina catalyst (Choi and Stenger, 2004) is used. The methanol and steam are fed simultaneously to the steam reformer where the steam reforming reactions take place to convert the reactant streams into hydrogen-rich gas. Furthermore, the product from the steam reformer is sent directly to the preferential oxidation reactor to reduce the CO concentration which can poison with anode of PEM fuel cell. However, the use of the water-gas shift reactor prior to the preferential oxidation reactor is considered for performance comparison of the systems.

The influences of operating parameters, i.e., temperature, steam-to-methanol (S/M) molar ratio, steam-to-carbon (S/C) molar ratio and oxygen-to-carbon (O/C) molar ratio on the performance of these two systems including methanol conversion, carbon monoxide conversion, energy consumption, volume of reactors (in term of weight of catalyst) and H₂ production, under steady state and isothermal conditions are investigated. .

5.1 Model validation

The validation of the reactor models (a steam reformer, a water-gas shift reactor and a preferential oxidation reactor) was carried out first to ensure that the developed mathematical models can well predict the performances of the reactors.

5.1.1 Methanol steam reformer

The mathematical model of the steam reformer is investigated as packed bed reactor, using the kinetic expressions taken from Pepply *et al.* (1999) whose kinetic and adsorption parameters are summarized in Table 4.1. They developed a comprehensive kinetic model for the reaction system over a wide range of temperature (up to 533 K) and pressure as high as 33 bar. The rate expressions of methanol steam reformer are combined with methanol-steam reforming (4.1), water-gas shift reaction (4.2) and methanol decomposition reaction (4.3) that occurred on a commercial Cu/ZnO/Al₂O₃ catalyst.

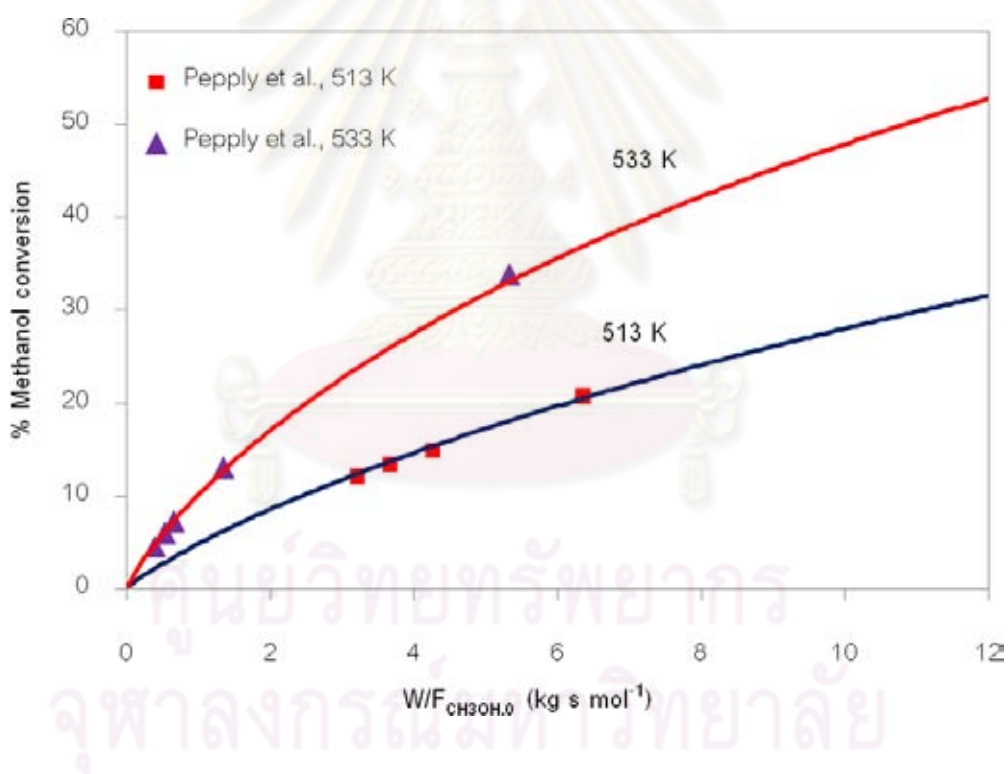


Figure 5.1 Comparison the methanol conversion between literature (Pepply *et al.*, 1999) and our prediction model at S/M molar ratio = 1, temperature = 513, 533 K and $P = 1.01$ bar.

The validity of the steam reformer is assessed by comparing our simulation results with reported experimental data from literature (Pepply *et al.*, 1999). Figure 5.1 shows the effect of temperature as a function of methanol conversion versus

a contact time measured in term of $W/F_{\text{CH}_3\text{OH},0}$ (weight of catalyst/ molar flow rate of methanol) in the range of 0-12 $\text{kg}_{\text{cat}} \text{ s mol}^{-1}$ at condition: pressure 1.01 bar and S/M molar ratio equal to 1. The points are experimental data of Pepply *et al.* and the solid lines are represented as our simulation results at 513 K and 533 K. It can be seen that the simulation results agreed well with experimental measurements.

5.1.2 Water-gas shift reactor

The rate expression occurred in this reactor is the water-gas shift reaction. Generally, this reaction is used to diminish the carbon monoxide concentration in hydrogen rich gas as product from steam reformer. In this work, the water-gas shift reaction is taken by Choi and Stenger (2003) as equation (4.5) on a commercial $\text{Cu/ZnO/Al}_2\text{O}_3$ catalyst. However, the mathematical model for water-gas shift reactor should be proved with the literature results clearly.

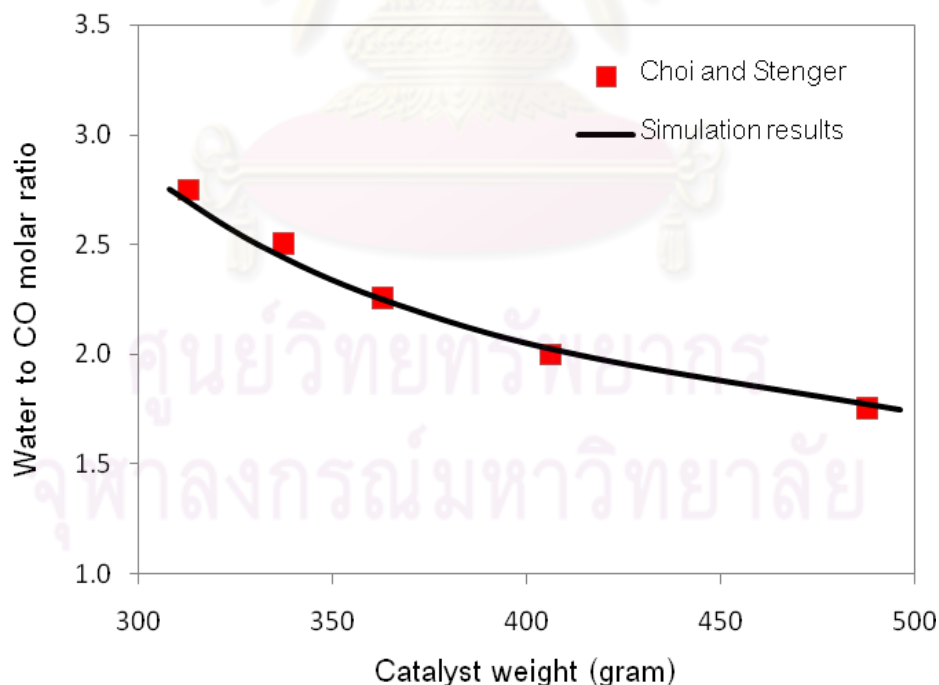


Figure 5.2 Comparison of simulation results between literature (Choi and Stenger ,2003) and our prediction model for 1 kW fuel cell to achieve 1 mol% of exiting CO concentration.

The simulation results from Choi and Stenger (2003) are considered at 1 kW fuel cell with molar flow rate of CO and H₂ as 11.1 and 22.2 mol/h, respectively. Figure 5.2 shows the comparison of the results achieved in this work with literature results that demonstrated the CO exiting the water-gas shift reactor as 1%mol in term of catalyst weight (gram) and water to CO molar ratio at 473 K. This comparison shows good agreement with the simulation results from literature.

5.1.3 Preferential oxidation reactor

The hydrogen rich gas is the main reactant for supplying to PEM fuel cell to generate the electricity. However, the carbon monoxide concentration of this stream should be reduced to ppm level to avoid the poisoning the PEM fuel cell anode so, preferential oxidation reactor is preferred. The rate expressions for preferential oxidation reactor in this study were performed by Choi and Stenger (2004) and after that, the expressions were further modified by Oliva *et al.* (2008) in order to avoid numerical problem and to facilitate convergence using the additional parameter **K** equal to 1×10^{-6} in equation of CO oxidation and H₂ oxidation. The rate expressions that occurred in this reactor combine with CO oxidation (4.7), hydrogen oxidation (4.8) and water-gas shift reaction (4.9) on Pt-Fe/ γ -alumina catalyst.

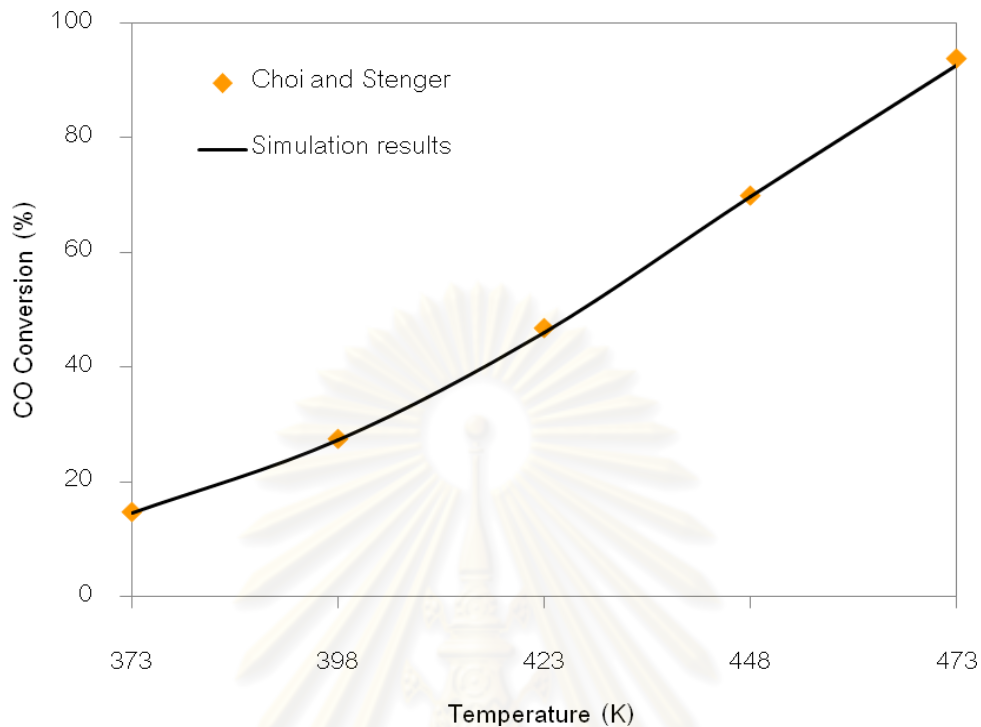


Figure 5.3 Comparison of the CO conversion between literature (Choi and Stenger, 2004) and our prediction model at various temperatures.

Figure 5.3 shows the effect of temperature on CO conversion using 50 g of catalysts, O_2/CO molar ratio of 1.2, hydrogen flow rate of 33 mol/h, 1%CO concentration and no water addition. The validity of preferential oxidation reactor is appraised by comparing our simulation results with literature results by Choi and Stenger (2004) which indicates a good agreement.

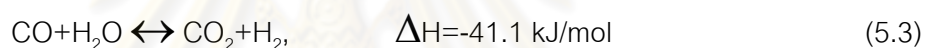
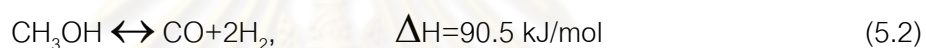
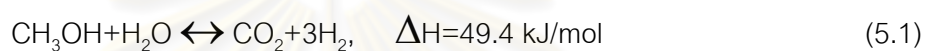
5.2 Thermodynamic analysis for the different reactors

This section presents the thermodynamic analysis of hydrogen production from methanol using steam reforming and water-gas shift reaction. The thermodynamic analysis was carried out to study the influence of temperature, S/M molar ratios and S/C molar ratios on methanol conversion for steam reformer, CO conversion for water-gas shift reactor and hydrogen production. In this work, the

suitable condition for steam reformer and water-gas shift reactor are determined to identify the limitation and effect from thermodynamic equilibrium on their maximum conversions.

5.2.1 Methanol steam reformer

The thermodynamic equilibrium of the steam reformer has been studied for methanol conversion and hydrogen production. The reactions concerned in this reformer for equilibrium condition are shown as following:



The gas species involved in the methanol steam reformer are CH_3OH , H_2O , CO , CO_2 and H_2 and conditions are evaluated in range of operating temperature from 300 to 580 K and the S/M molar ratio from 1.0 to 3.0 at atmospheric pressure.

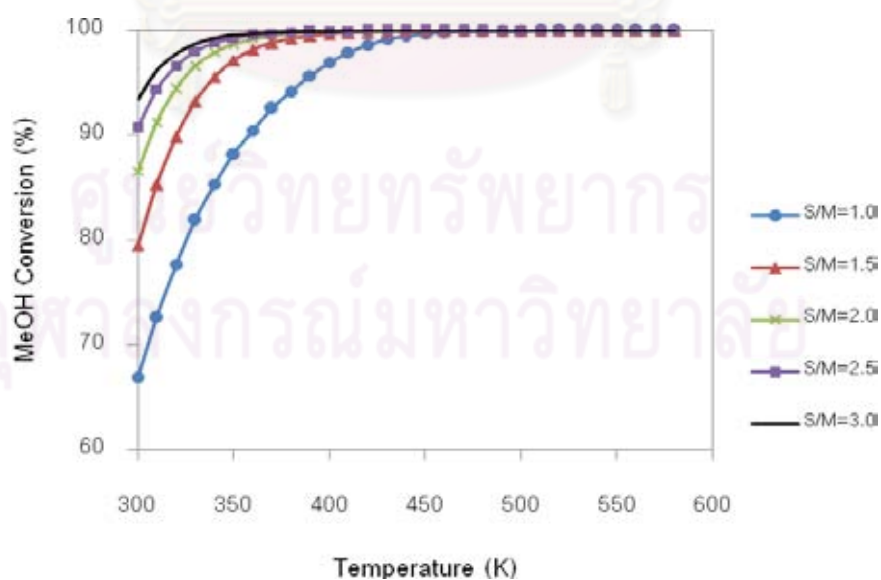


Figure 5.4 Effect of temperature and S/M ratio on the equilibrium conversion of methanol in the steam reformer.

Figure 5.4 shows the equilibrium conversion of methanol from the methanol steam reformer with the various temperature and S/M ratio. The equilibrium conversion of methanol rapidly increases with temperature and S/M ratio. As a result, the complete conversion of methanol was accomplished as temperature and S/M ratio are higher than 400 K and 1, respectively.

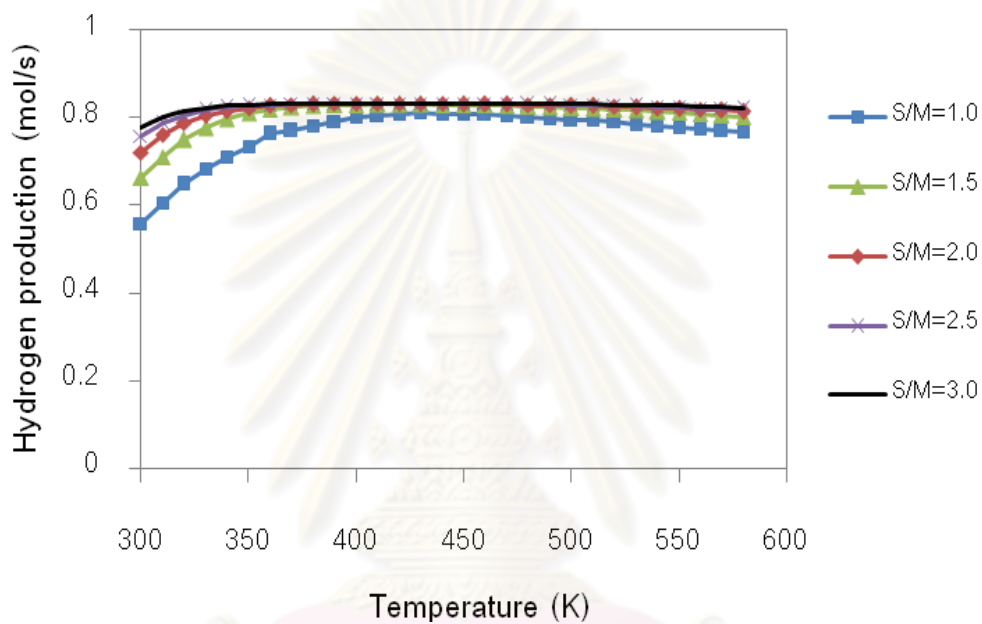


Figure 5.5 Effect of temperature and S/M molar ratio on the hydrogen production in the steam reformer.

The effects of temperature and S/M molar ratio on the hydrogen production are shown in Figure 5.5. It can be seen that hydrogen production is improved with increasing temperature but levels off after $T = 425$ K. The S/M molar ratio shows strong effect at low temperature but slight effect at higher temperature on hydrogen production. In term of the equilibrium concentration of hydrogen as shown in Figure 5.6, it declined at a higher S/M molar ratio due to the reverse water-gas shift reaction that favorably occurs at high temperature. At the same time, the CO concentration extremely rised with increasing temperature and the S/M molar ratio lower than 1.5 as shown in Figure 5.7.

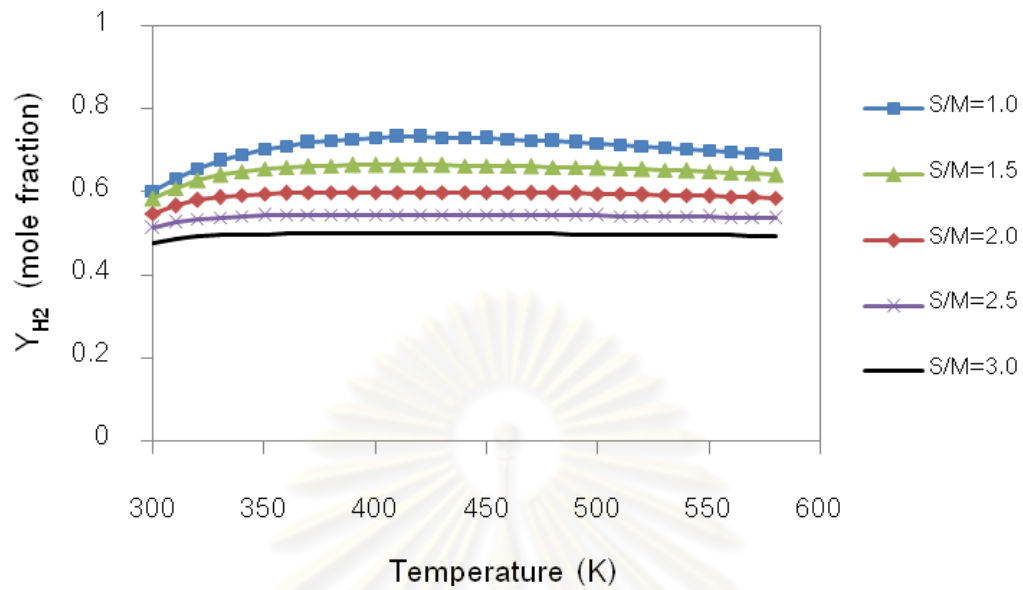


Figure 5.6 Effect of temperature and S/M molar ratio on the equilibrium concentration of hydrogen in the steam reformer.

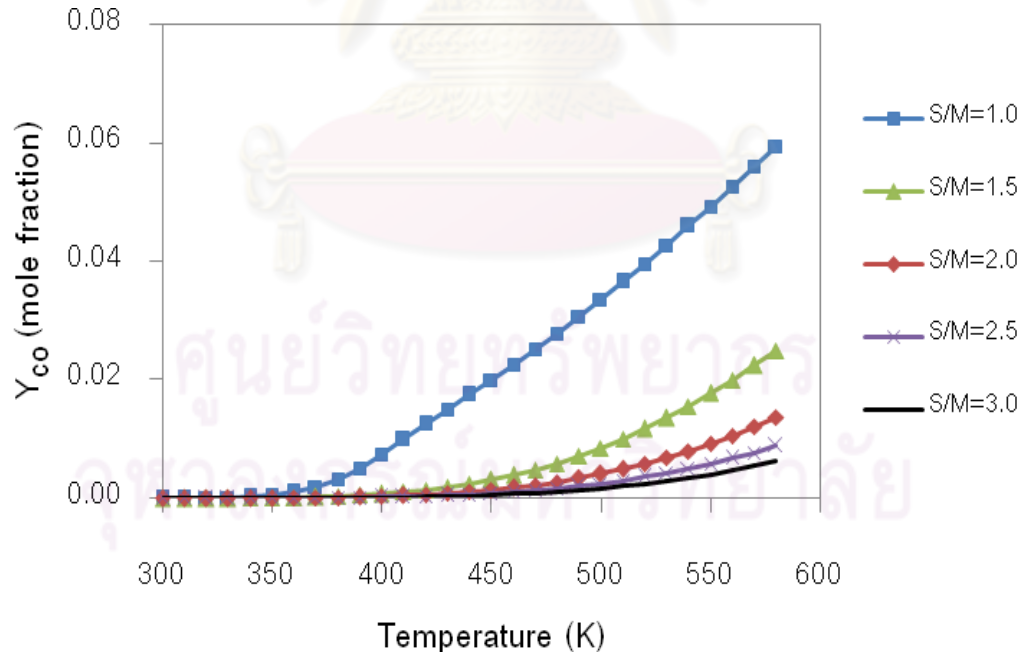


Figure 5.7 Effect of temperature and S/M molar ratio on the equilibrium concentration of carbon monoxide in the steam reformer.

5.2.2 Water-gas shift reactor

The water-gas shift reactor is one type of the CO-cleanup process that can convert the carbon monoxide to hydrogen by reacting with steam. To investigate the thermodynamic equilibrium of the water-gas shift reactor, the feed composition of the water gas shift reactor was based on the equilibrium gas composition from the steam reformer. The main reaction taking place in the water gas shift reactor is as follow:



The gas species involved in the water-gas shift reactor are CO, H₂O, CO₂ and H₂ and conditions are evaluated in range of operating temperature from 300 to 450 K and S/C molar ratio from 1.0 to 3.0 at atmospheric pressure.

The condition from the steam reformer at S/M molar ratio = 1.5 and 450 K which considered the composition of product streams to feed steam for the water-gas shift reactor are provided in Table 5.1 below:

Table 5.1 The mole fraction of component in feed stream to the water-gas shift reactor.

Species	CH ₃ OH	H ₂ O	CO	CO ₂	H ₂
Mole fraction	Trace amount	0.1144	0.0032	0.2190	0.6633

The equilibrium conversion of carbon monoxide in the water-gas shift reactor as functions of S/C molar ratio and temperature was shown in Figure 5.8. The conversion of carbon monoxide slightly changed with rising S/C molar ratio. On the contrary, the conversion extremely reduced with increasing temperature as shown in Figure 5.9.

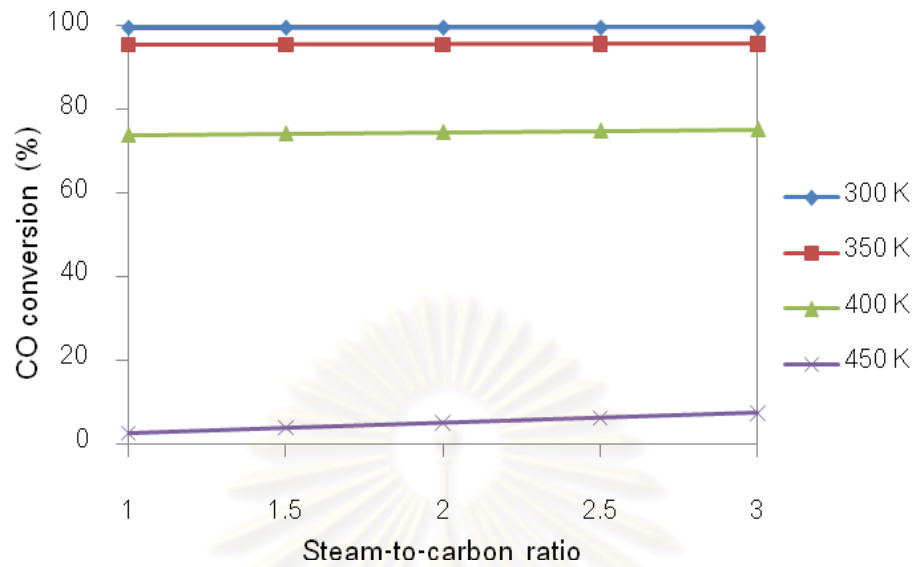


Figure 5.8 Effect of S/C molar ratio and temperature on the equilibrium conversion of carbon monoxide in the water-gas shift reactor.

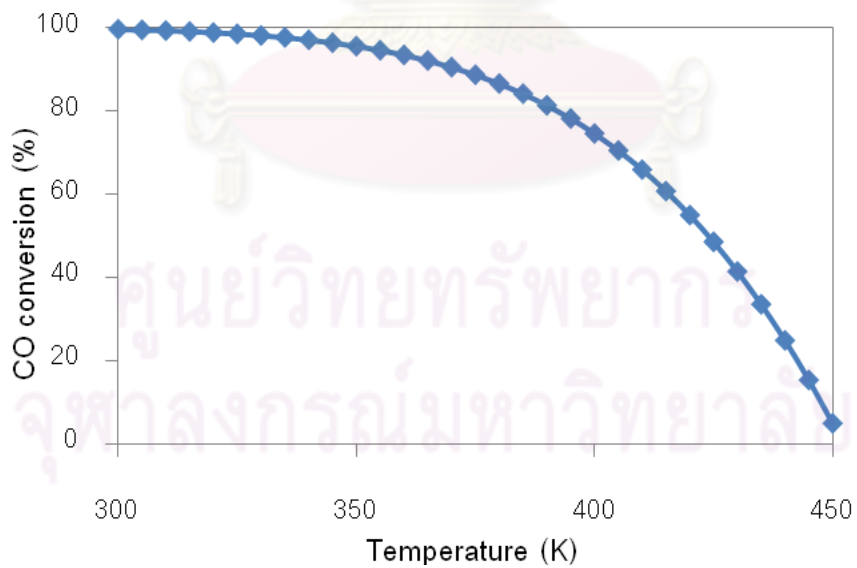


Figure 5.9 Effect of temperature on the equilibrium conversion of carbon monoxide in the water-gas shift reactor at S/C molar ratio=2.0.

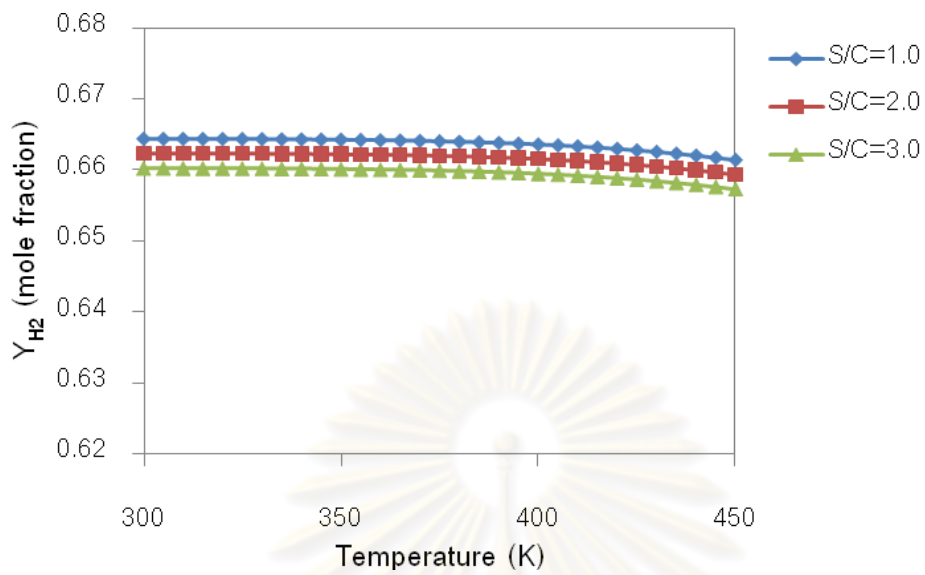


Figure 5.10 Effect of temperature and S/C molar ratio on the equilibrium concentration of hydrogen in the water-gas shift reactor.

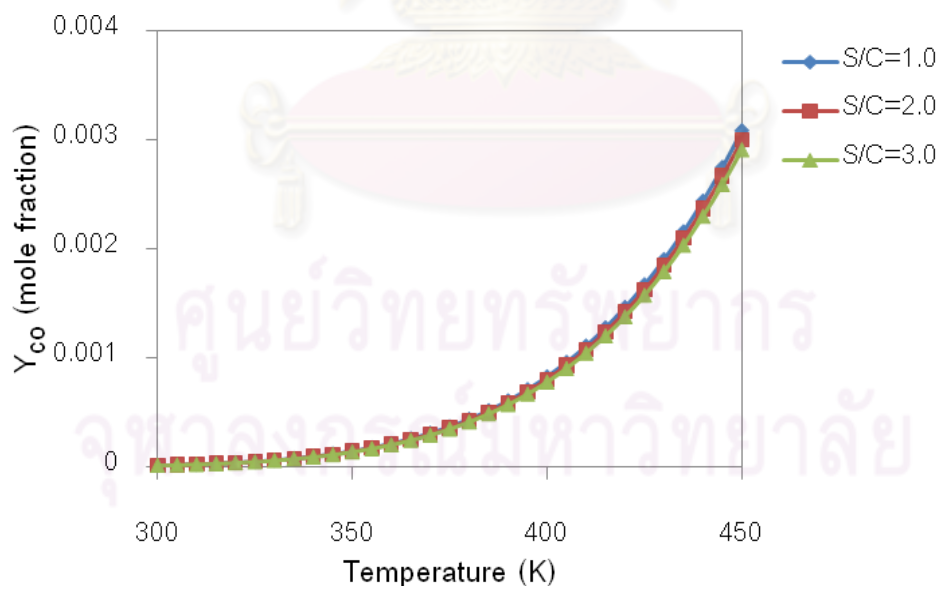


Figure 5.11 Effect of temperature and S/C molar ratio on the equilibrium concentration of carbon monoxide in the water-gas shift reactor.

Figures 5.10 and 5.11 show the fraction of hydrogen and carbon monoxide, respectively at various temperatures and S/C molar ratios. At the higher S/C molar ratio, the hydrogen concentration vaguely decreased caused by the dilution with the excessive steam. At increasing temperature resulted in a raise in CO concentration. But S/C molar ratio do not effect.

5.3 Simulation results of SYS I

The on-board fuel processor is preferred to produce the hydrogen directly using methanol as fuel source. For SYS I, the fuel processor is combined with steam reformer and preferential oxidation reactor that are modeled as the plug flow reactors. The steam reformer and preferential oxidation reactor are packed with $\text{Cu/ZnO/Al}_2\text{O}_3$ catalyst (Peppley, 1999) and $\text{Pt-Fe}/\gamma\text{-alumina}$ catalyst (Choi and Stenger, 2004), respectively. A schematic for SYS I is shown in Figure 5.12.

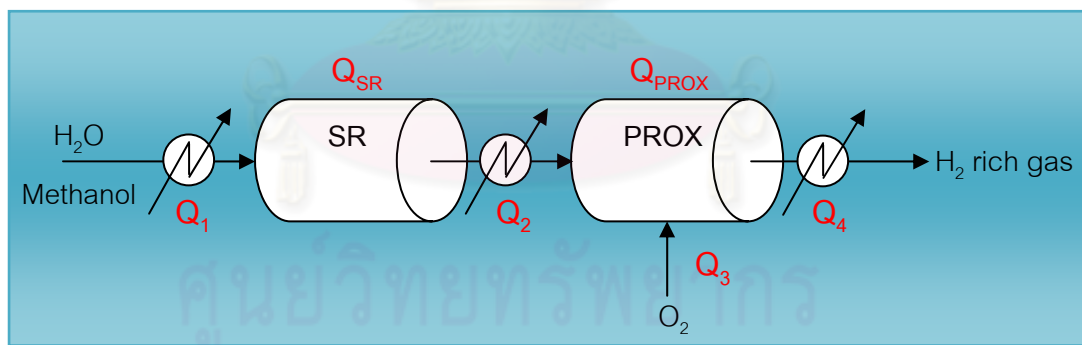


Figure 5.12 Schematic diagram of SYS I consisting of the steam reformer and the preferential oxidation reactor.

5.3.1 Steam reformer in SYS I

The feeds composing of methanol and steam are fed in the steam reformer for conversion into hydrogen-rich gas via methanol steam reforming reactions. For SYS I, the steam-to-methanol molar ratio (S/M) of 2.0 and the various temperatures ranging from 433 to 533 K are considered. The simulation results at this condition are shown in Figures 5.13, 5.14 and 5.15 as methanol conversions, hydrogen productions and, the outlet CO concentrations, respectively in terms of catalyst loadings and reformer temperatures. It is observed that the rising of reformer temperature leads to increases of the methanol conversion, hydrogen and also the outlet CO concentration. The increasing of CO outlet with higher temperatures is undesired because the CO content in H_2 -rich stream can poison anode of PEMFC, leading to reduction of power generation efficiency. Catalyst loading decreased with increasing temperature to achieve the target MeOH conversion for example, at 95.00% MeOH conversion, the catalyst loading required are 56.90, 36.10 and 23.30 kg for 503, 513 and 523 K, respectively. This trend of catalyst loading also occurred for hydrogen production and CO outlet concentration undoubtedly.

However, to design the steam reformer for SYS I, the methanol conversion should be considered to produce the suitable process for SYS I. The MeOH conversions are selected at 95.00%, 97.00%, 99.00% and 99.50%. At these conversions, the corresponding values of catalyst loadings, hydrogen production and CO outlet concentration are compared.

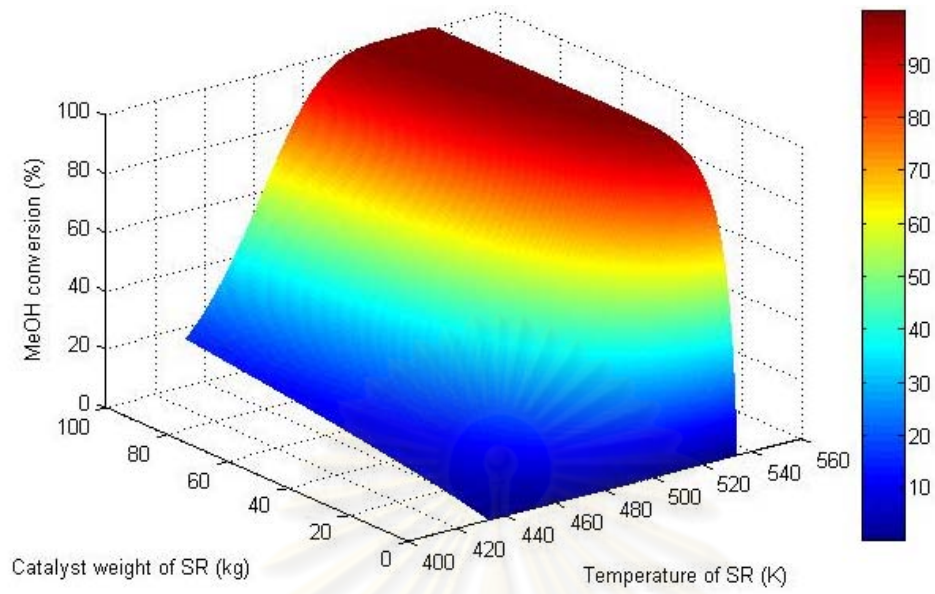


Figure 5.13 Methanol conversion of steam reformer for SYS I.

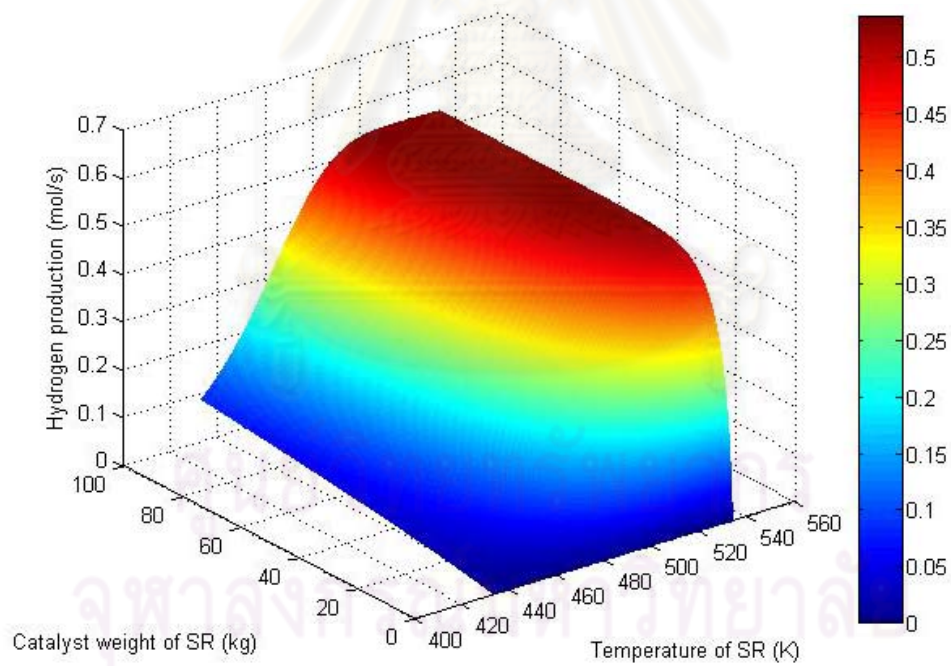


Figure 5.14 Hydrogen production rate of steam reformer for SYS I.

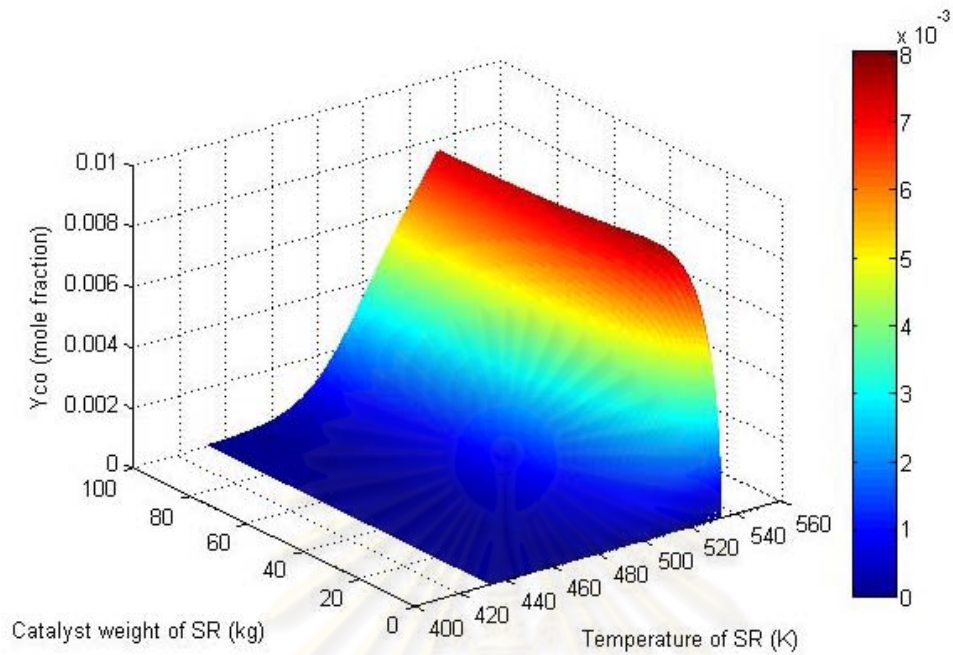


Figure 5.15 CO concentration in product gas from steam reformer for SYS I.

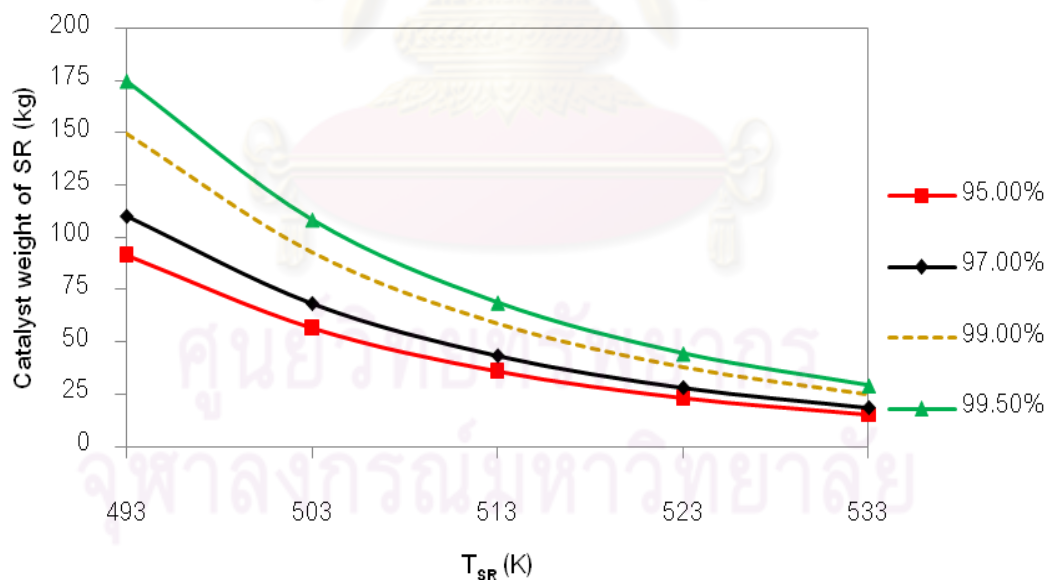


Figure 5.16 Catalyst weights for SR vs. temperature of SR at different methanol conversions for SYS I.

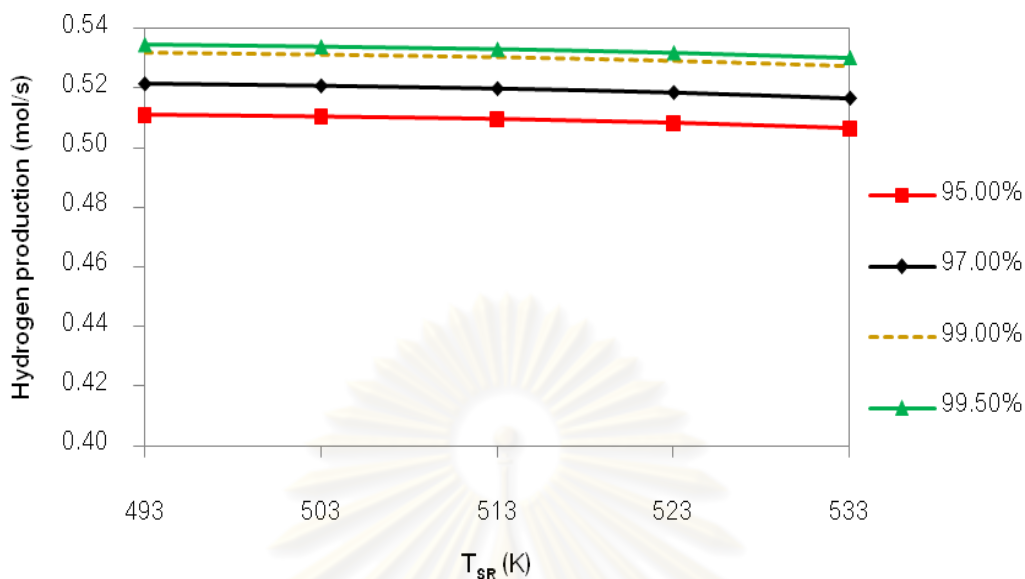


Figure 5.17 Hydrogen production rate vs. temperature of SR at different methanol conversions for SYS I.

Figures 5.16, 5.17 and 5.18 present the effect of temperature of steam reformer on catalyst weight, hydrogen production and CO concentration in SR outlet, respectively for different methanol conversions. Figure 5.16 shows that the catalyst loadings are declined with increasing reformer temperature as same as the hydrogen production that slightly drops as demonstrated in Figure 5.17. However, the CO concentration in SR outlet stream is rapidly increased with the higher reformer temperature as shown in Figure 5.18 because CO component is a by-product from the methanol decomposition reaction that favored at high temperature. While the water-gas shift reaction that converts CO to CO₂ is favored at low temperature. In terms of methanol conversions, the volume of reformer is highly increased as well as hydrogen production and CO concentration at higher methanol conversions.

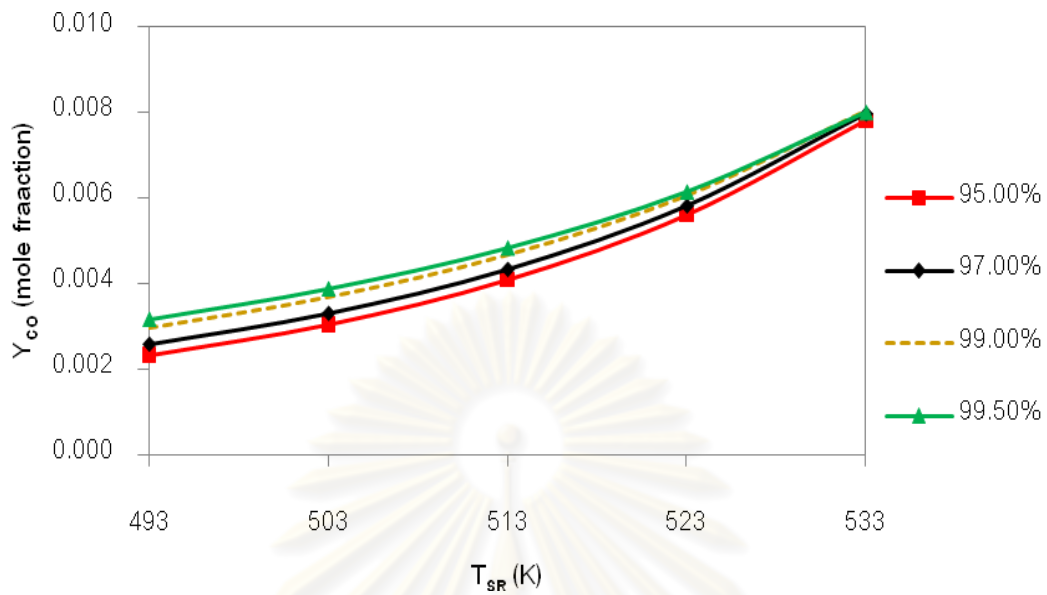


Figure 5.18 Mole fraction of CO in SR outlet vs. temperature of SR at the different methanol conversions for SYS I.

The methanol conversion is specified at 99.50% to produce the sufficient hydrogen for supplying to PEMFC and to ensure trace amount of methanol present in the product gas. The different temperatures are selected at 513, 523 and 533 K to find out the suitable systems for SYS I. The compositions of outlet stream from steam reformer at 99.50% are presented in Table 5.2 for different reformer temperatures and these conditions are subsequently used as feeds for PROX reactor. It should be noted that the reactions that occur in the steam reformer are extremely endothermic. Therefore, the heat supply for the steam reformer is essentially investigated. The heat requirement for the steam reformer (SYS I) is summarized in Table 5.3.

Table 5.2 Mole fraction of components in outlet streams from the steam reformer SYS I.

T_{SR} (K)	CH ₃ OH	H ₂ O	CO	CO ₂	H ₂
513	Trace amount	0.2062	4.827E-03	0.1946	0.5934
523	Trace amount	0.2075	6.141E-03	0.1933	0.5921
533	Trace amount	0.2094	7.996E-03	0.1914	0.5902

Table 5.3 Heat requirement for operating steam reformer (SYS I).

	Power consumption for SR (kW)		
	513 K	523 K	533 K
Reformer temperature	513 K	523 K	533 K
Preheat MeOH and H ₂ O (Q ₁)	26.23	26.42	26.61
Heat supply for reactions (Q _{SR})	10.78	10.90	11.03

5.3.2 CO clean-up process in SYS I

For SYS I, the preferential oxidation reactor is provided for decrement of CO concentration in H₂ rich stream from the steam reformer. The reverse water-gas shift, CO and H₂ oxidation reactions are taken place in this reactor. In this study, the target of CO concentration in outlet stream from PROX reactor is set at 50 ppm (Ouzounidou *et al.*, 2009) to avoid toxic for anode in PEMFC. The oxygen-to-carbon molar ratio (*O/C*) is fixed at 2.0 and the reactor temperatures are varied from 423 to 523 K. The composition of reformates from the different reformer temperatures as shown in Table 5.2 are delivered to PROX reactor.

The simulation results for PROX reactor are shown in Figures 5.19 and 5.20 as catalyst loading and hydrogen production, respectively at different reactor temperatures. To achieve the CO content at 50 ppm, the catalyst loading is reduced with increasing reactor temperature as shown in Figure 5.19. The reduction of volume reactor in term of catalyst at higher temperature is decreased the prospect of the remaining O₂ reacting with H₂ in H₂ oxidation reaction. Figure 5.20 shows the effect of reactor temperature on hydrogen production at CO content 50 ppm. Some hydrogen is consumed in PROX reactor but the extent at high temperature is lower than that at low temperature due to the limiting of catalyst loading where the H₂ oxidation occurred (after CO depleted).

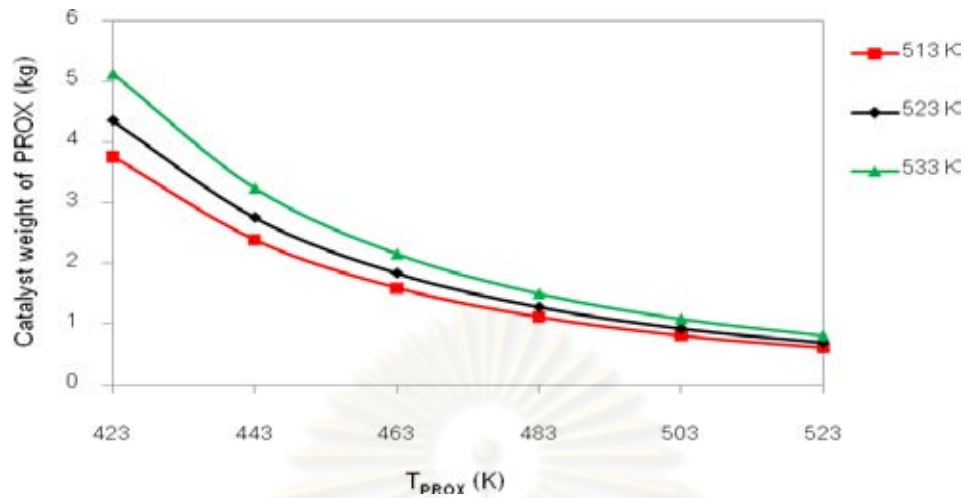


Figure 5.19 Catalyst weight of PROX reactor vs. temperature of PROX reactor at different conditions from the steam reformer ($[\text{CO}]_{\text{out}} = 50$ ppm).

The reactions that occurred in the PROX reactor are highly exothermic reactions but air inlet need to be heated up before feeding to the reactor so some heat is required. The heat requirement around the PROX reactor is shown in Figure 5.21. The result shows that the additional heat to preheat air is very small when compared with the heat releases from reactions.

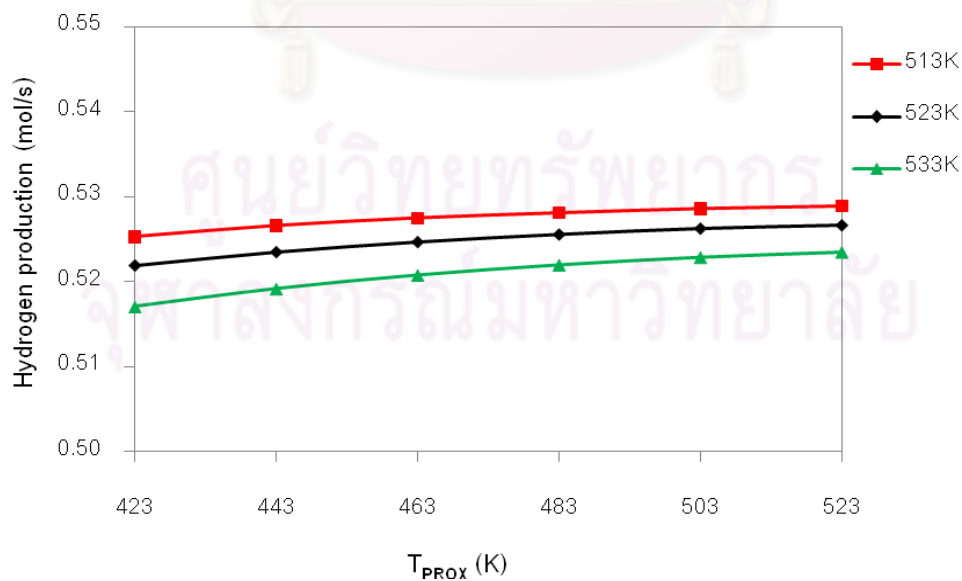


Figure 5.20 Hydrogen production of PROX reactor vs. temperature of PROX reactor at the different conditions from the steam reformer ($[\text{CO}]_{\text{out}} = 50$ ppm).

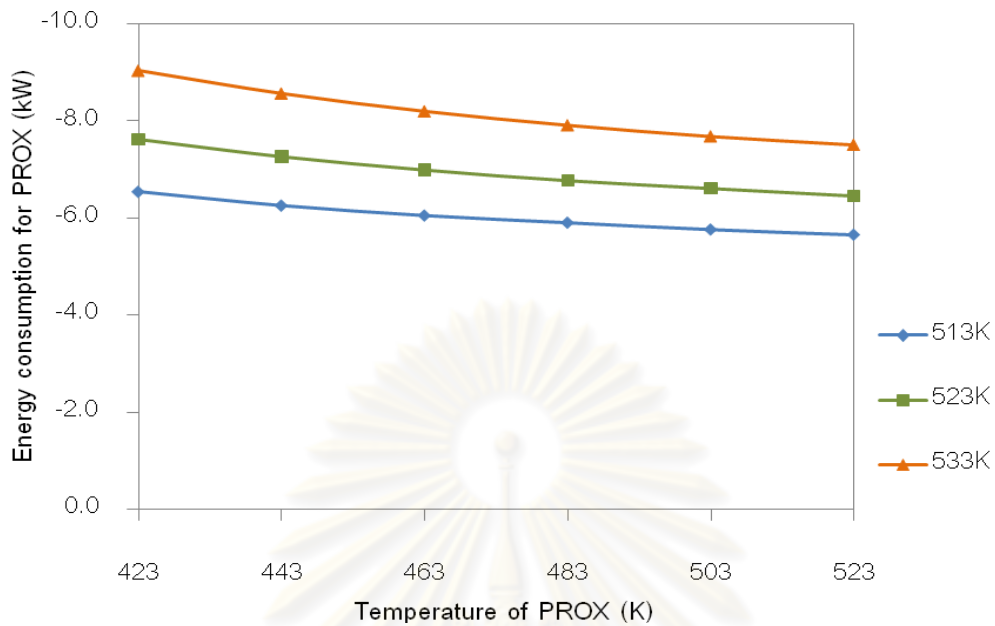


Figure 5.21 Energy consumption for the PROX reactor.

The final hydrogen production achieved from SYS I are enough to generate the electricity on PEMFC 50 kW at every temperatures of PROX reactor. So, to select the suitable condition of SYS I, the total catalyst weights and energy consumption of SYS I are investigated. Figure 5.22 shows the total catalyst loading for SYS I and Figure 5.23 shows the energy consumption of SYS I at different temperatures of steam reformer and PROX reactor. The reformer temperature of 533 K presents the lowest total catalyst weight as well as energy consumption for SYS I at the various PROX reactor temperatures.

ศูนย์วิจัยทรัพยากร
จุฬาลงกรณ์มหาวิทยาลัย

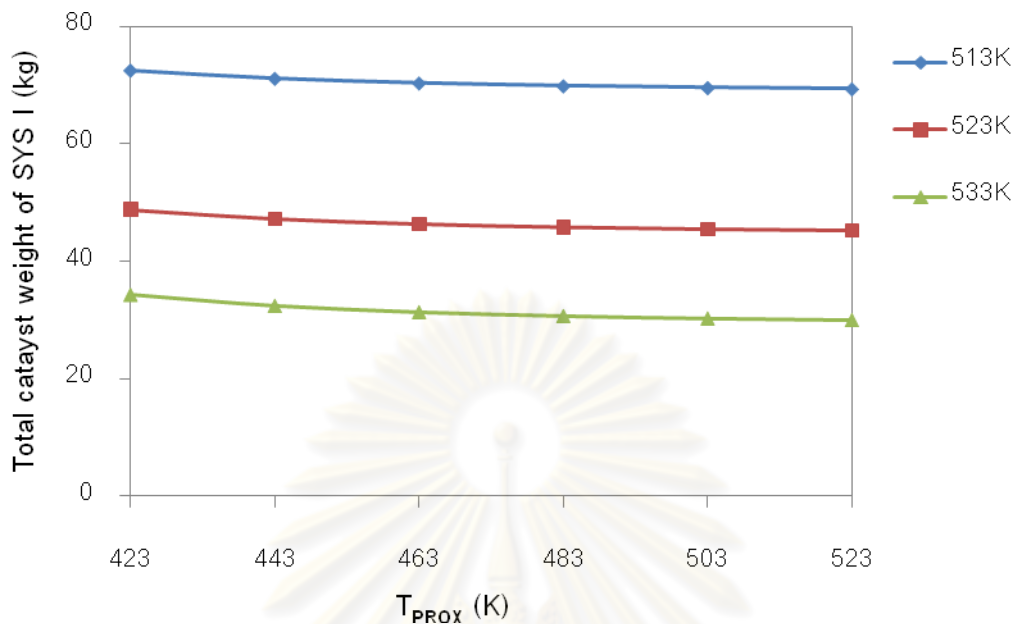


Figure 5.22 Total catalyst weight for SYS I vs. temperature of PROX reactor at different feed conditions from the steam reformer.

Finally, the total catalyst weights of SYS I are more strongly affected by temperature of steam reformer than temperature of PROX reactor so, reformer temperature at 533 K was considered. However, the temperatures of PROX reactor also influence total catalyst weight and energy consumption for SYS I as shown in Figure 5.22 and 5.23. Operation at T_{SR} 533 K and T_{PROX} 423 K presents the lowest energy consumption but in term of catalyst loading it is higher than that at the same T_{SR} . So, the selection of a suitable condition for SYS I should consider about the area on the vehicles to make sure that enough for on-board fuel processor and also the heat supply for systems.

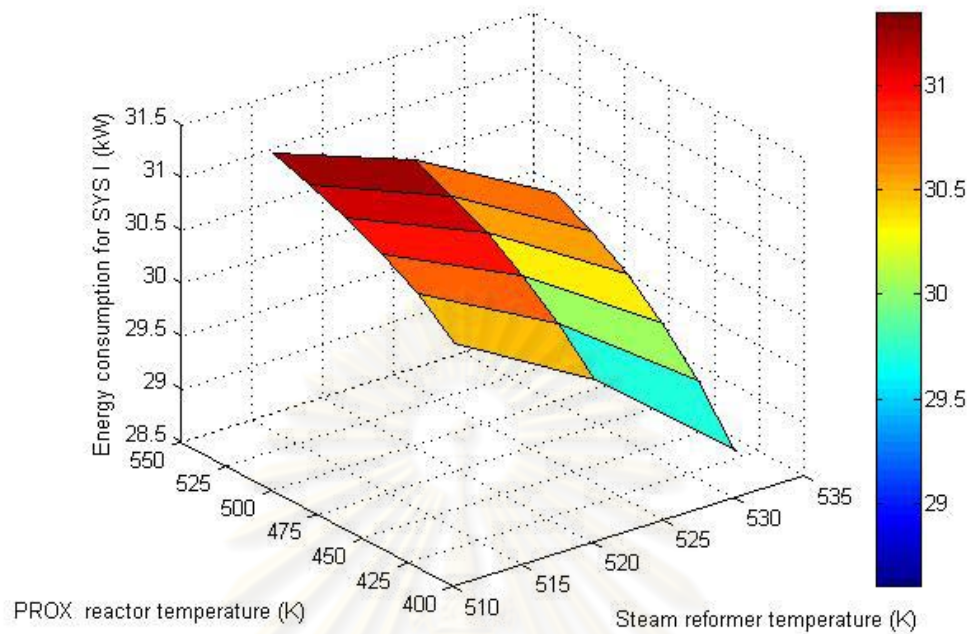


Figure 5.23 Energy consumption for SYS I vs. temperature of PROX reactor and the steam reformer.

5.4 Simulation results of SYS II

In this section, the performance of SYS II comprising of the steam reformer, WGS reactor and PROX reactor is investigated. The designs of steam reformer and PROX reactor are similar to those of SYS I. The WGS reactor is packed with Cu/ZnO/Al₂O₃ catalyst (Choi and Stenger, 2003). A schematic diagram of SYS II is shown in Figure 5.24

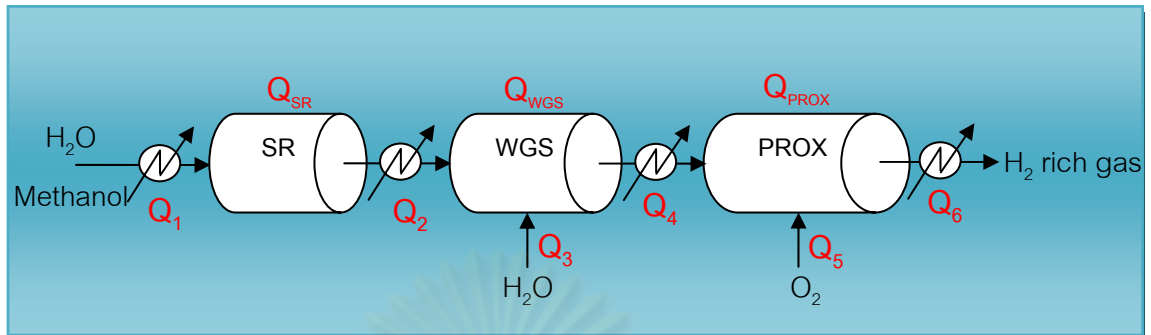


Figure 5.24 Schematic diagram of SYS II consisting of the steam reformer, water-gas shift reactor and the preferential oxidation reactor.

5.4.1 Steam reformer in SYS II

For SYS II, the *S/M* molar ratio of 1.5 is kept at and the various temperatures from 433 to 533 K are considered. At this condition, the simulation results are presented in Figures 5.25, 5.26 and 5.27 as methanol conversions, hydrogen productions and, the outlet CO concentrations, respectively at different values of catalyst weights and reformer temperatures. The results follow the same trend as those of SYS I but the hydrogen production is lower while CO concentration is higher due to the decrease of *S/M* molar ratio from 2.0 in SYS I to 1.5 in this system. These results agree well with the trend reported in the thermodynamic analysis of methanol steam reformer as shown in Figs. 5.5 and 5.7. The rising *S/M* molar ratio has influenced on the increasing hydrogen production rate and the decreasing CO concentration obviously. However, the CO conversion slightly drops at the same weight catalyst. It is not in line with thermodynamic equilibrium as the reaction may be influenced by the decomposition reaction.

To compare between SYS I and SYS II, the MeOH conversions for SYS II are selected at 95.00%, 97.00%, 99.00% and 99.50% as same as SYS I. At these conversions are evaluated in terms of catalyst loadings, hydrogen production and CO outlet concentration.

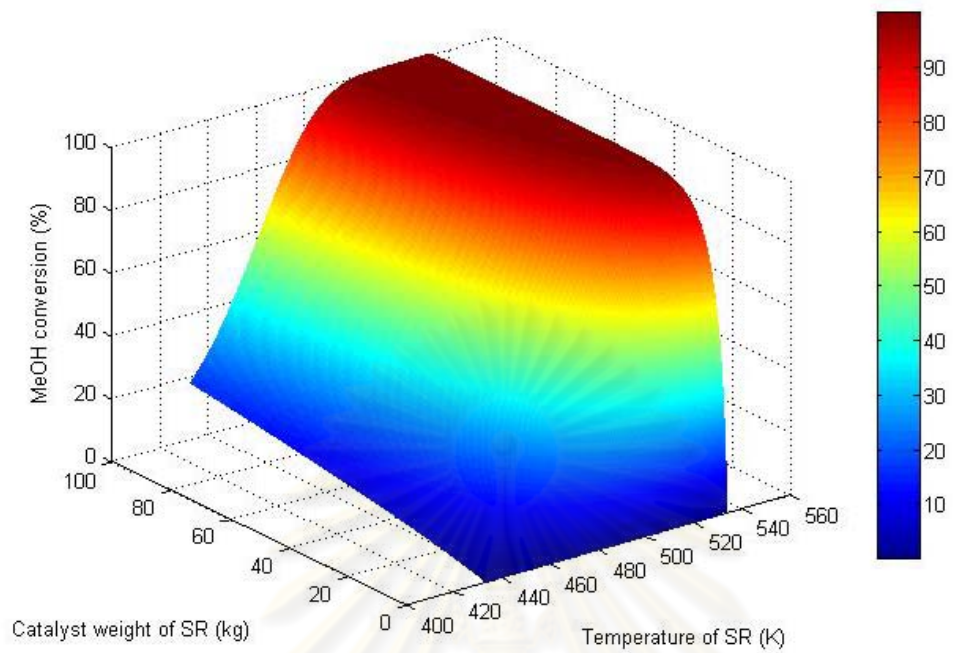


Figure 5.25 Methanol conversion of steam reformer for SYS II.

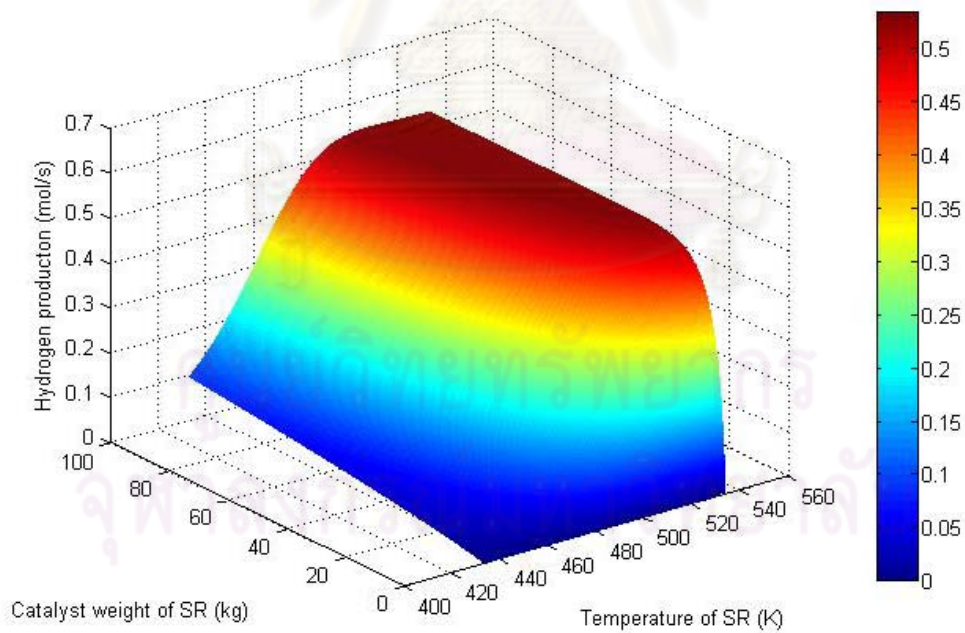


Figure 5.26 Hydrogen production rate of steam reformer for SYS II.

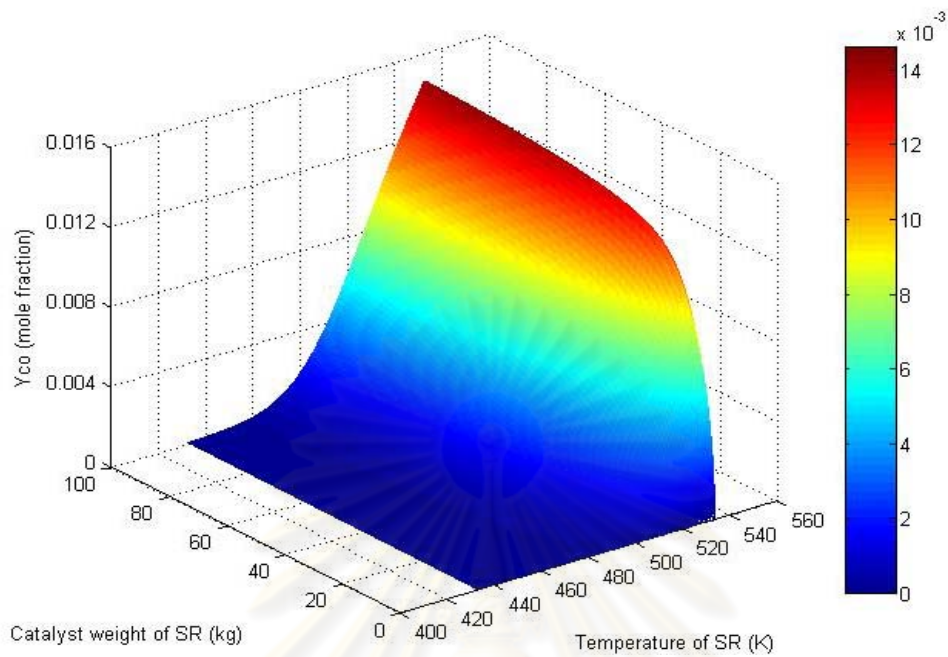


Figure 5.27 CO concentration in gas product of steam reformer for SYS II.

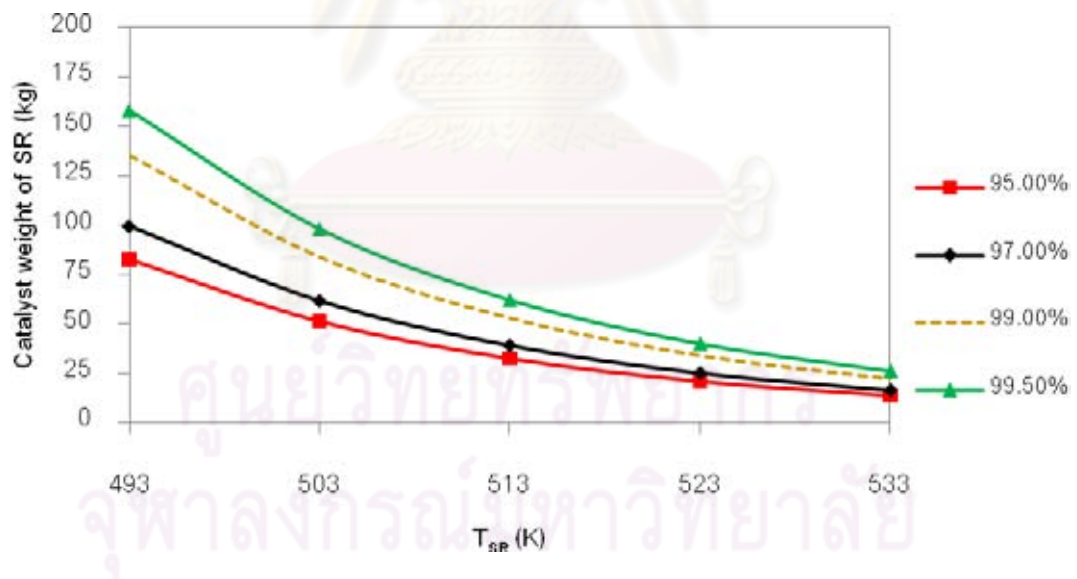


Figure 5.28 Catalyst weights for SR vs. temperature of SR at different methanol conversions for SYS II.

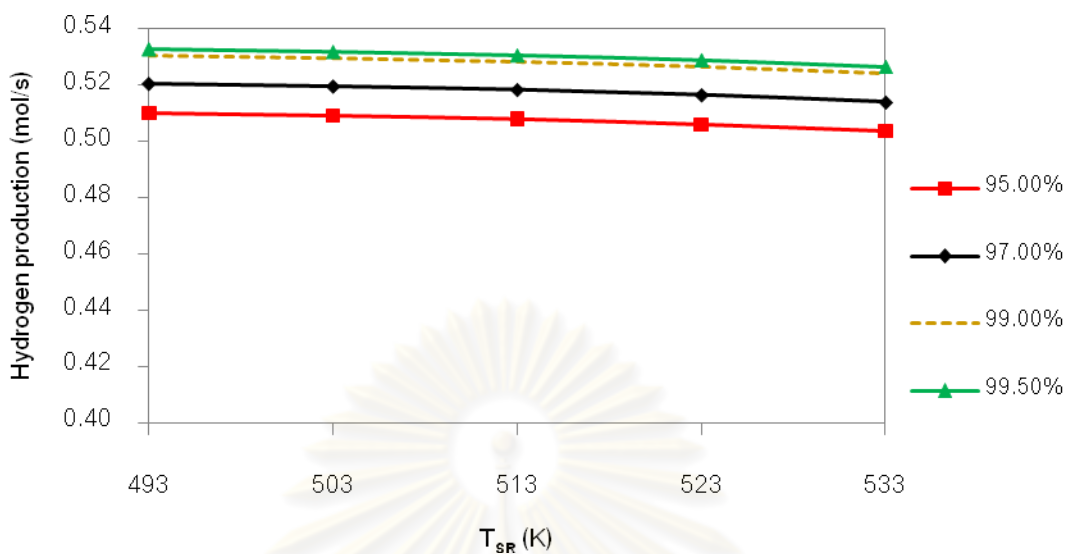


Figure 5.29 Hydrogen productions in SR outlet vs. temperature of SR at different methanol conversions for SYS II.

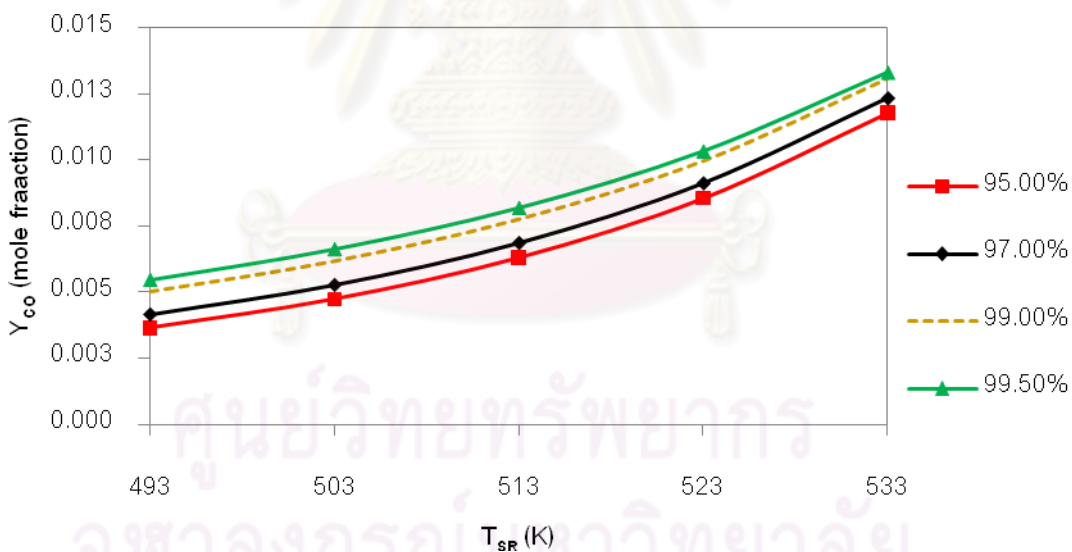


Figure 5.30 Mole fraction of CO in SR outlet vs. temperature of SR at different methanol conversions for SYS II.

Figures 5.28, 5.29 and 5.30 present the effect of temperature of steam reformer on catalyst weight, hydrogen production and CO concentration in SR outlet (SYS II), respectively for different levels of methanol conversions. These simulation results show the similar trends of decreasing catalyst loading and hydrogen production

but increasing CO concentration when increasing reformer temperature as reported earlier for SYS I.

In terms of methanol conversions, the volume of reformer is highly increased same as hydrogen production and CO concentration at higher methanol conversions. However, at the same conversion between SYS I and SYS II, they show that the catalyst loading for SYS II are less than that for SYS I for example, at 95% MeOH conversion and T_{SR} 533 K, catalyst loadings are 15.3 and 13.7 kg for SYS I and SYS II, respectively.

The methanol conversion is specified at 99.50% as SYS I to produce the sufficient hydrogen for supplying to PEMFC and the different temperatures at 513, 523 and 533 K are considered to select the suitable systems for SYS II. The compositions of outlet stream from steam reformer at 99.50% are presented in Table 5.4 with the different reformer temperatures and these conditions are used as feeds for WGS reactor. The steam reformer displays the highly endothermic reaction so, some heat need to supply the steam reformer sufficiently. The heat requirement for the steam reformer (SYS II) is shown in Table 5.5.

Table 5.4 Mole fraction of components in outlet streams from the steam reformer SYS II.

T_{SR} (K)	CH ₃ OH	H ₂ O	CO	CO ₂	H ₂
513	Trace amount	0.1207	8.193E-03	0.2134	0.6566
523	Trace amount	0.1228	1.033E-02	0.2113	0.6544
533	Trace amount	0.1258	1.330E-02	0.2083	0.6515

Table 5.5 Heat requirement for operating steam reformer (SYS II).

Reformer temperature	Power consumption for SR (kW)		
	513 K	523 K	533 K
Preheat MeOH and H ₂ O (Q_1)	21.64	21.80	21.96
Heat supply for reactions (Q_{SR})	10.86	10.99	11.18

5.4.2 CO clean-up processes in SYS II

Besides the PROX reactor provided as a CO removal process, the WGS reactor is presented in SYS II to reduce the CO concentration before feeding to the subsequent PROX. Additional steam is fed to WGS reactor in an amount of 0.09 mol/s so that the overall S/M is the same for both SYS I and SYS II.

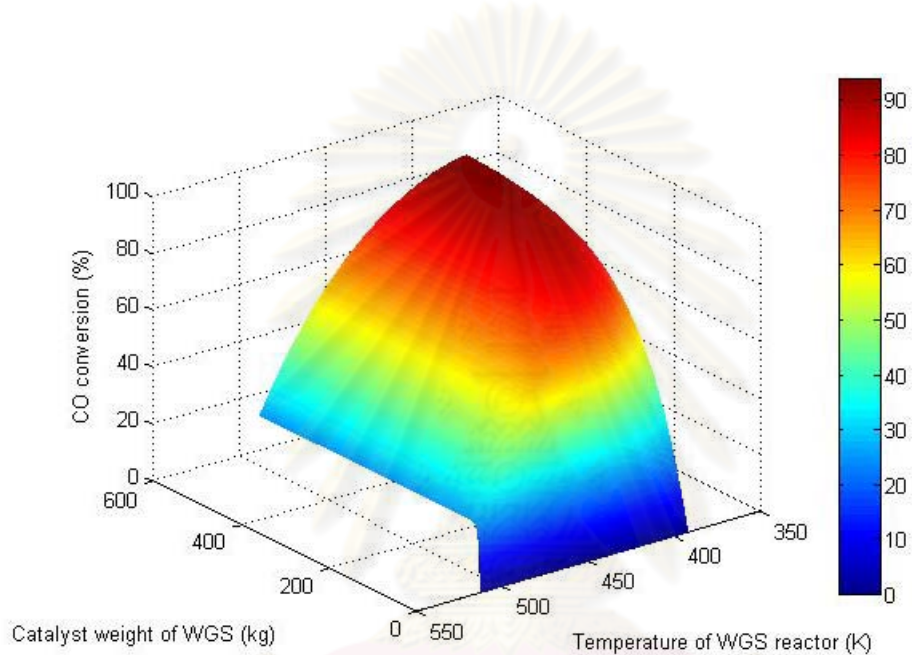


Figure 5.31 CO conversion vs. catalyst weight of WGS reactor at various temperatures of WGS reactor ($T_{SR} = 513$ K).

The CO conversion is presented in Figure 5.31. The feed is based on the outlet composition from the steam reformer at 513 K. It should be noted that the similar trends are observed for the feed compositions from the cases with $T_{SR} = 523$ and 533 K. At higher temperature of WGS, the equilibrium conversion of CO is low but the reaction rate is very fast. On the contrary, reaction rate is slow at low temperature while the CO conversion is elevated. These results agreed well with the thermodynamic analysis of WGS reactor.

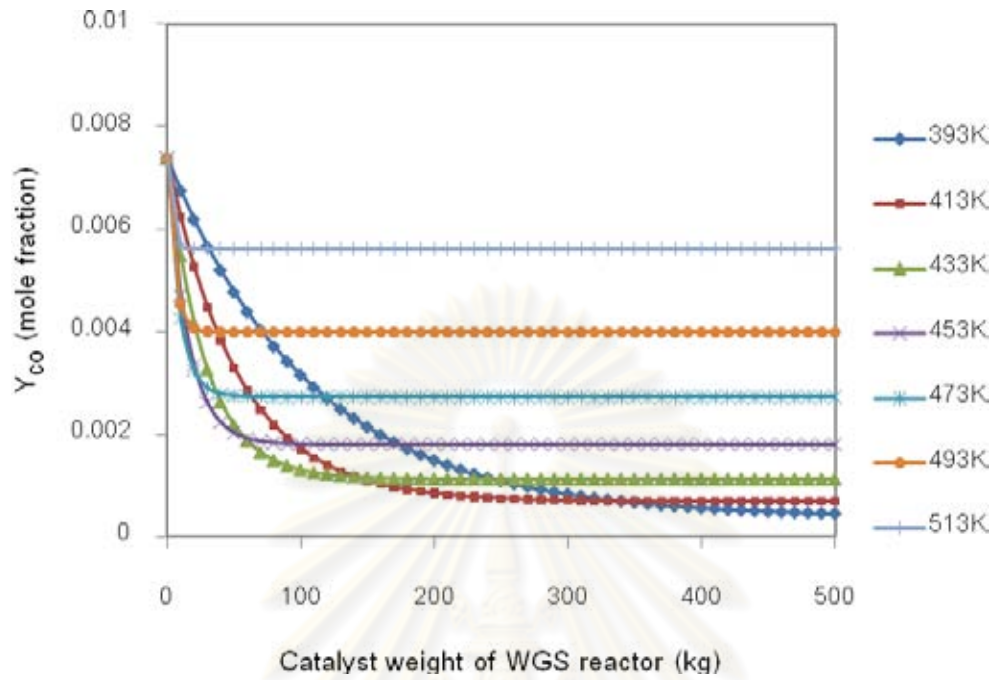


Figure 5.32 CO concentration vs. catalyst weight of WGS reactor at various temperatures of WGS reactor ($T_{SR} = 513K$).

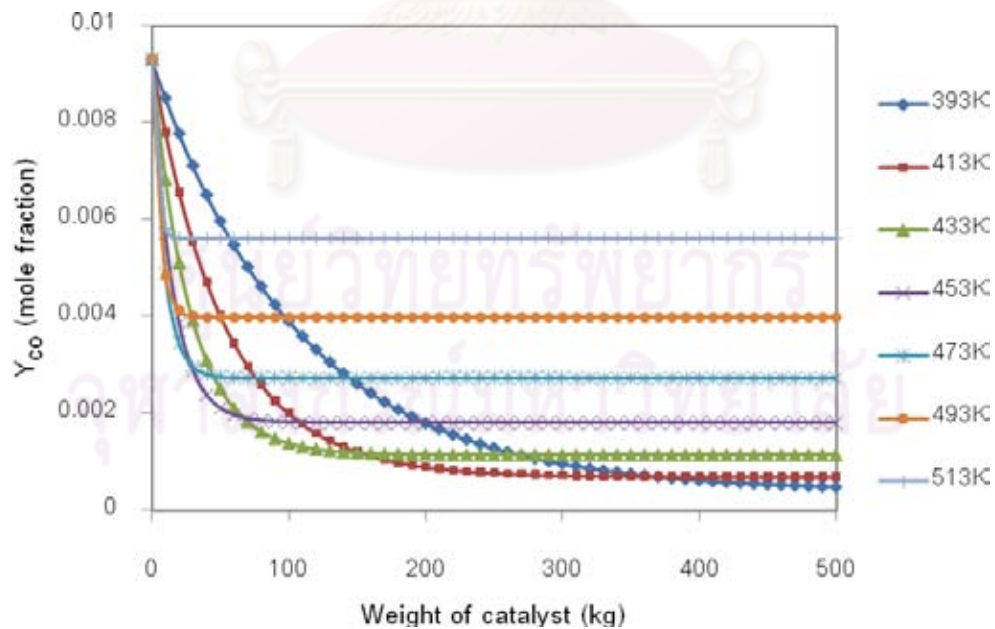


Figure 5.33 CO concentration vs. catalyst weight of WGS reactor at various temperatures of WGS reactor ($T_{SR} = 523K$).

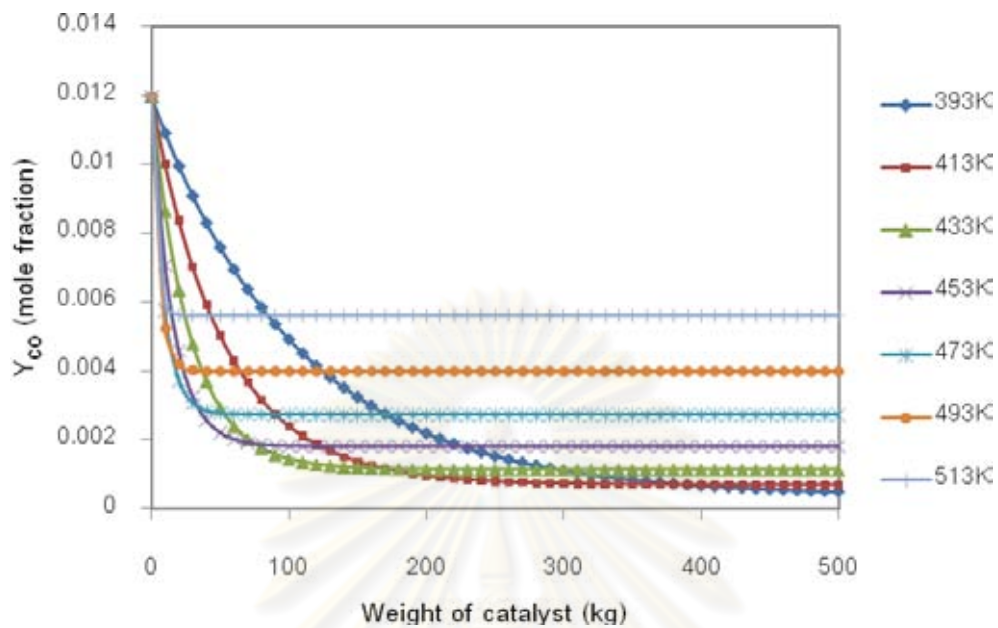


Figure 5.34 CO concentration vs. catalyst weight of WGS reactor at various temperatures of WGS reactor ($T_{SR} = 533K$).

Figures 5.32, 5.33 and 5.34 show the CO concentrations as a function of catalyst weight of WGS reactor fed by reformat from the steam reformer operated at different temperatures. It is observed that the lowest CO content at every reformer temperatures are about 5×10^{-4} (mole fraction) at catalyst loadings 500 kg. Due to the volume of reactor is very large at the lowest content so, the CO contents need to be considered. Two levels of CO concentration in the WGS product of 0.003 and 0.004 are considered for comparison.

จุฬาลงกรณ์มหาวิทยาลัย

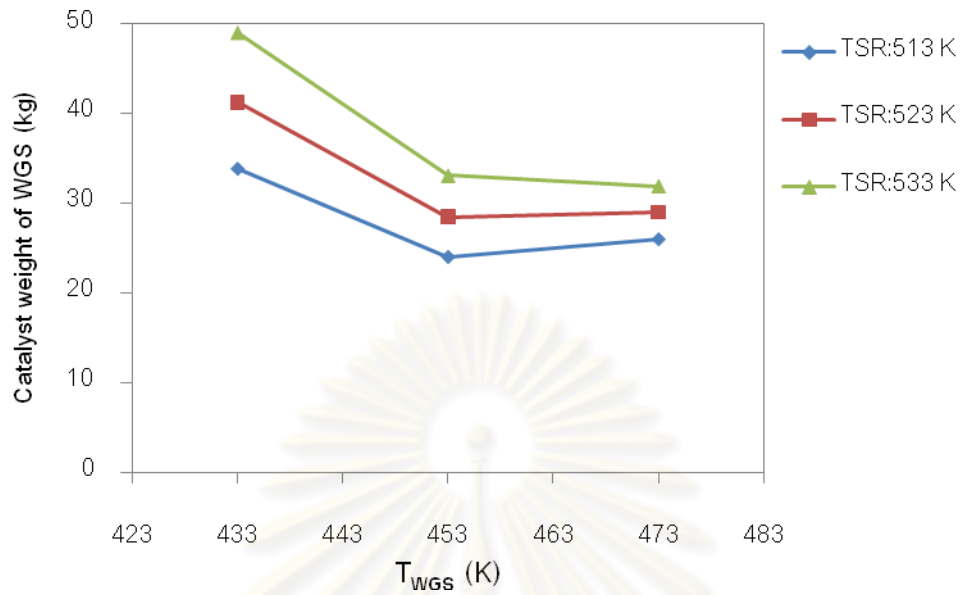


Figure 5.35 Catalyst weights of the WGS reactor vs. WGS temperatures at different reforming temperature feeds ($[CO]_{out\ WGS}=0.003$).

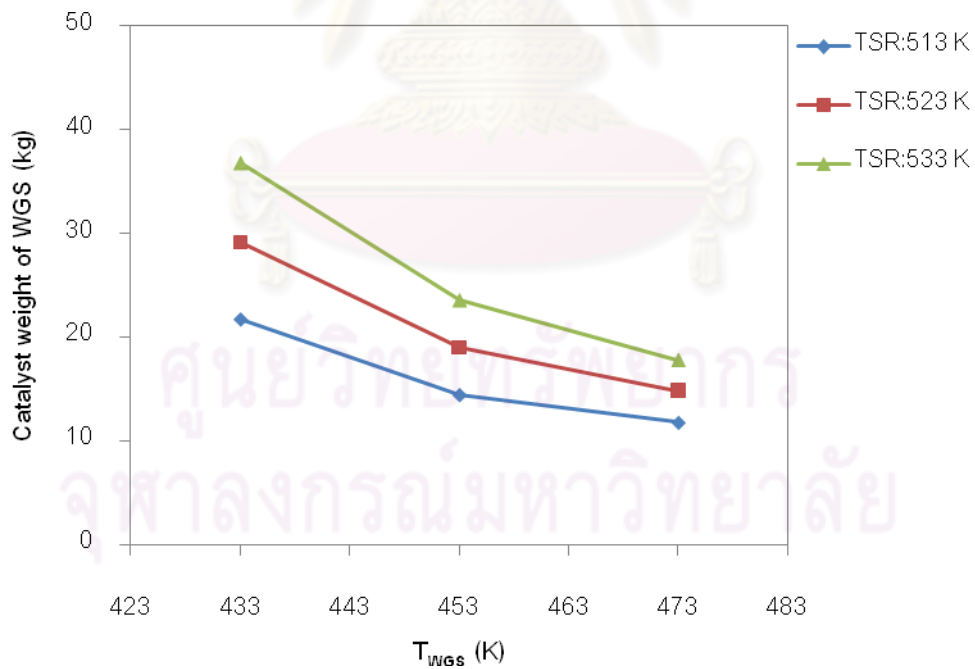


Figure 5.36 Catalyst weights of the WGS reactor vs. WGS temperatures at different reforming temperature feeds ($[CO]_{out\ WGS}=0.004$).

To obtain the CO concentration at 0.003 and 0.004, the values of the catalyst loadings for WGS reactor are determined at different temperatures of WGS reactor ($T = 433, 453$ and 473 K) as shown in Figures 5.35 and 5.36, respectively.

The comparison shows that the catalyst loadings at X_{CO} of 0.003 are higher than that at X_{CO} of 0.004 because the former requires more effort to reduce CO concentration to the desired value. The effect of increasing CO concentration on hydrogen production rate is shown in Figure 5.37. The hydrogen production rates are almost the same for different WGS temperatures because the compositions for each of CO outlet concentration are similar. The gas product from WGS reactor becomes the feed of PROX reactor. Tables 5.6 and 5.7 summarize the feed compositions of PROX reactor from the different temperatures of WGS reactor (433, 453 and 473 K) at concentration of CO of 0.003 and 0.004, respectively.

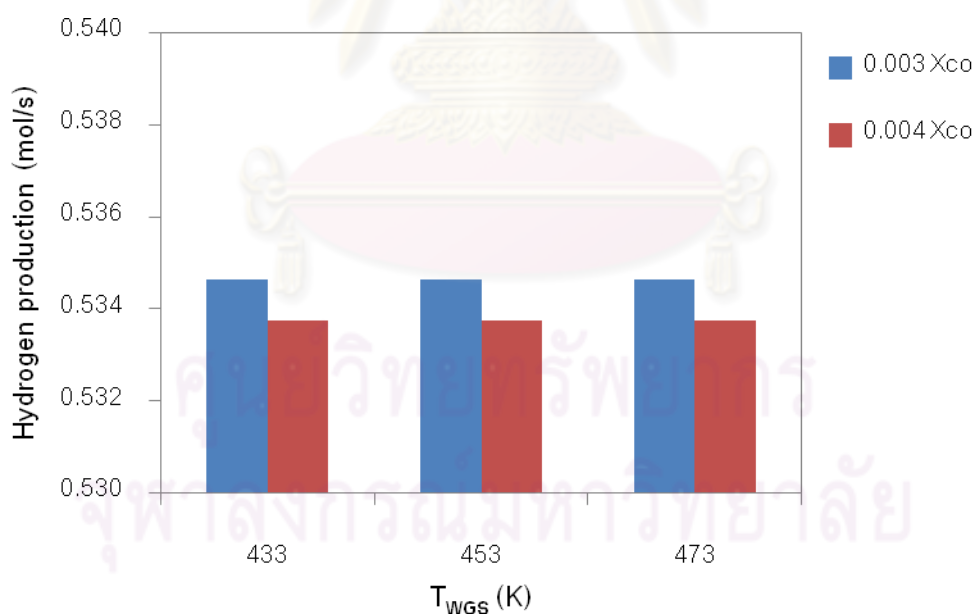


Figure 5.37 Hydrogen production rate for the WGS reactor at various temperatures of the WGS reactor for CO concentrations of 0.003 and 0.004.

The water-gas shift reaction is exothermic and carried out in WGS reactor. However, the additional water for WGS reactor needs to be preheated before feeding into the reactor. The exothermic heat from reaction can sufficiently supply for preheating water. Figures 5.38 and 5.39 show the energy consumption for WGS reactor ($Q_2+Q_3+Q_{WGS}$) at different CO outlet contents of 0.003 and 0.004, respectively. The results show the energy consumption of WGS reactor for cases of different temperatures of WGS reactor and steam reformer. At lower temperature, the energy released is higher than at elevated temperature due to the different temperature between steam reformer and WGS reactor.

Table 5.6 Mole fraction of components in outlet streams from the WGS reactor for SYS II at $X_{CO} = 0.003$.

T_{SR} (K)	T_{WGS} (K)	CO	H ₂ O	CO ₂	H ₂
513	433	0.0030	0.2046	0.1966	0.5958
	453	0.0030	0.2046	0.1966	0.5958
	473	0.0030	0.2046	0.1966	0.5958
523	433	0.0030	0.2046	0.1967	0.5957
	453	0.0030	0.2046	0.1967	0.5957
	473	0.0030	0.2046	0.1967	0.5957
533	433	0.0030	0.2046	0.1966	0.5958
	453	0.0030	0.2047	0.1966	0.5958
	473	0.0030	0.2047	0.1966	0.5958

Table 5.7 Mole fraction of components in outlet streams from the WGS reactor for SYS II at $X_{CO} = 0.004$.

T_{SR} (K)	T_{WGS} (K)	CO	H ₂ O	CO ₂	H ₂
513	433	0.0040	0.2056	0.1956	0.5948
	453	0.0040	0.2056	0.1956	0.5948
	473	0.0040	0.2056	0.1956	0.5948
523	433	0.0040	0.2056	0.1957	0.5947
	453	0.0040	0.2056	0.1957	0.5947
	473	0.0040	0.2056	0.1957	0.5947
533	433	0.0040	0.2057	0.1956	0.5947
	453	0.0040	0.2057	0.1956	0.5947
	473	0.0040	0.2057	0.1956	0.5947

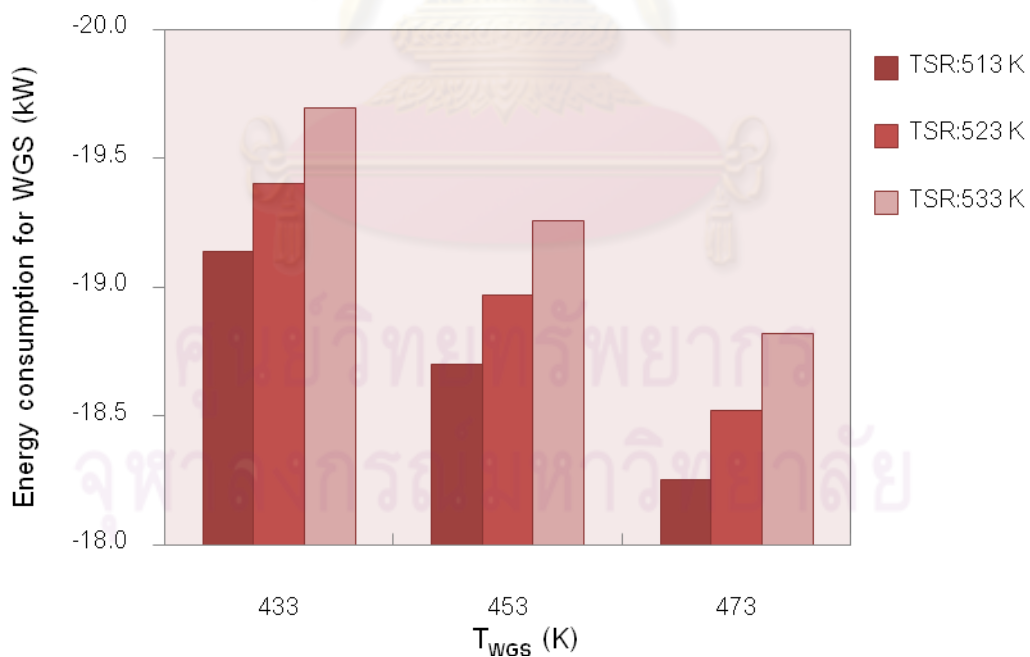


Figure 5.38 Energy consumption for the WGS reactor at $X_{CO} = 0.003$.

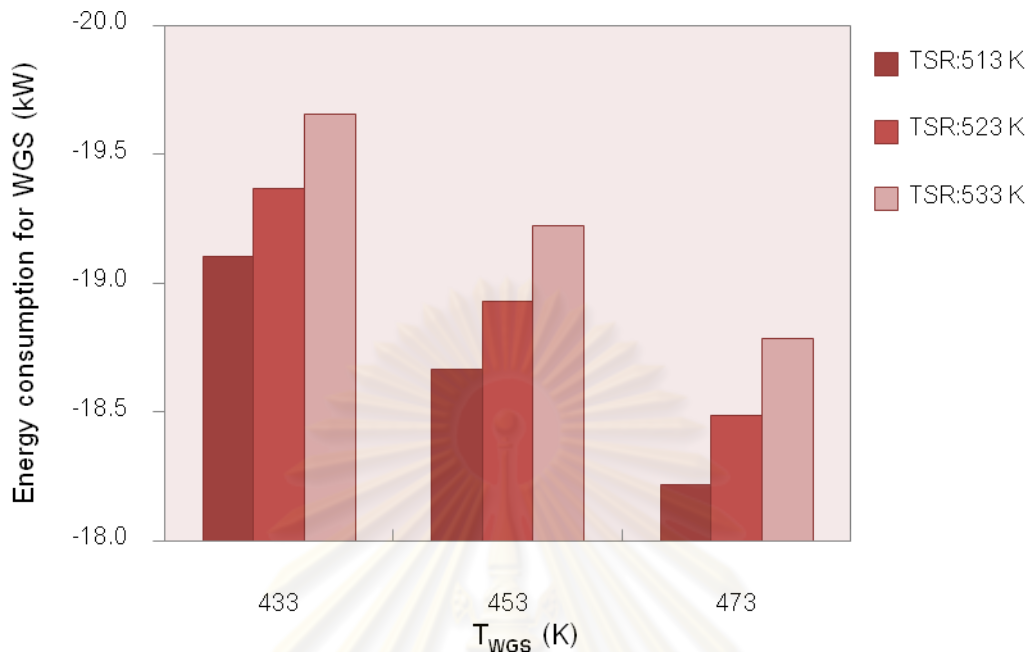


Figure 5.39 Energy consumption for the WGS reactor at $X_{CO} = 0.004$.

The components from Table 5.6 and 5.7 are fed to the PROX reactor for final reduction of CO concentration for PEMFC. In PROX reactor, CO is converted to CO_2 with additional O_2 by CO oxidation reaction. Moreover, some H_2 are consumed by O_2 via H_2 oxidation reaction that causes H_2 loss in outlet streams of PROX reactor. In this study, the target of CO concentration in outlet stream from PROX reactor is set at 50 ppm (Ouzounidou *et al.*, 2009) same as SYS I to avoid toxic for anode side in PEMFC and O/C molar ratio is fixed at 2.0 and the reactor temperatures are varied from 423 to 523 K.

Figures 5.40 and 5.41 show the effect of temperature of PROX reactor on catalyst loadings for PROX reactor at the different CO inlet concentrations. As you can see that the catalyst loadings of PROX reactor are dependent on temperature of WGS reactor obviously because the inlet streams from WGS reactor present the same composition with the different temperatures of WGS reactor. However, the reformer temperatures has slight effect on catalyst weight of PROX reactor.

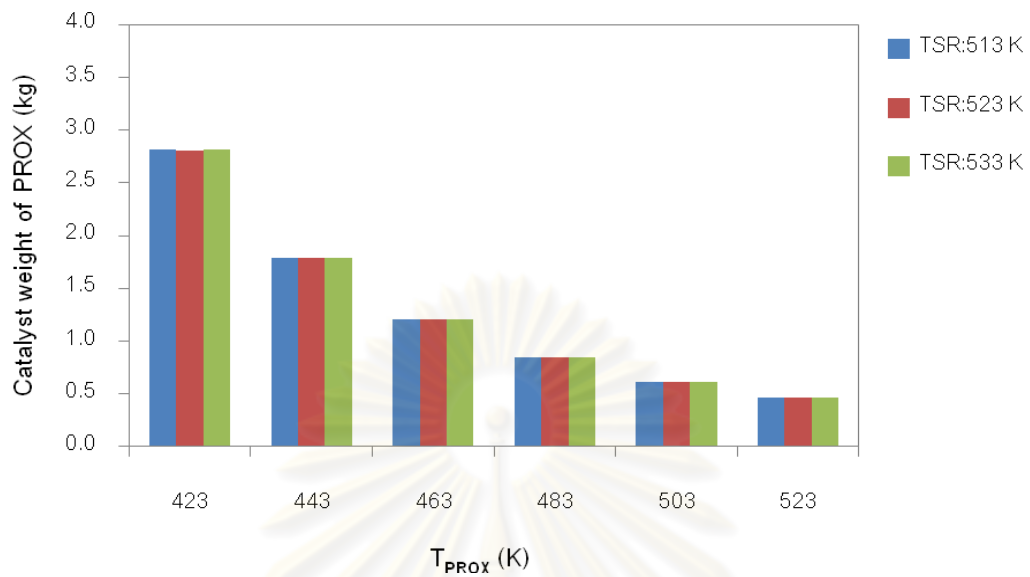


Figure 5.40 Catalyst weight of PROX reactor vs. T_{PROX} at X_{CO} inlet of 0.003 ($[\text{CO}]_{\text{out}} = 50$ ppm).

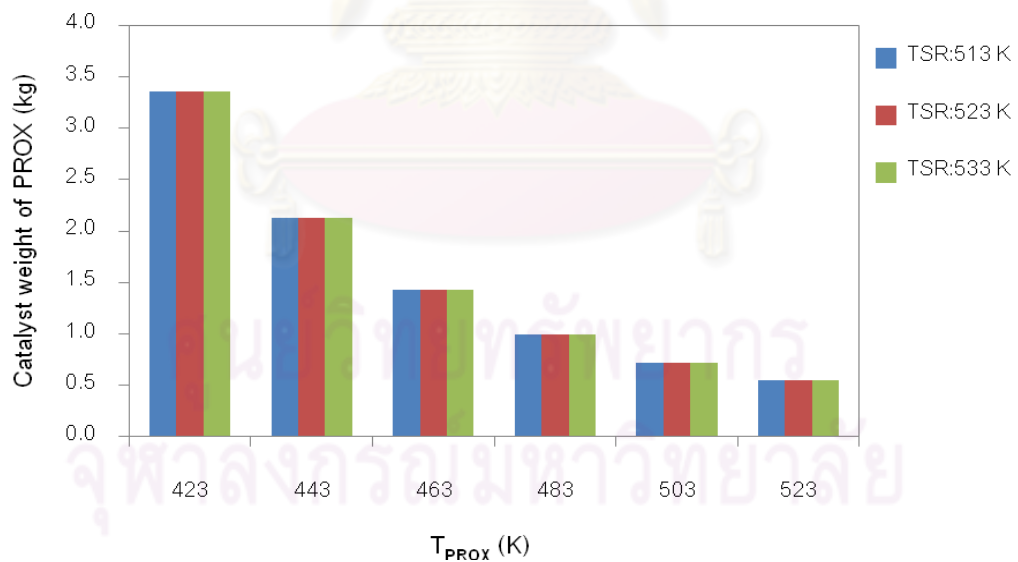


Figure 5.41 Catalyst weight of PROX reactor vs. T_{PROX} at X_{CO} inlet of 0.004 ($[\text{CO}]_{\text{out}} = 50$ ppm).

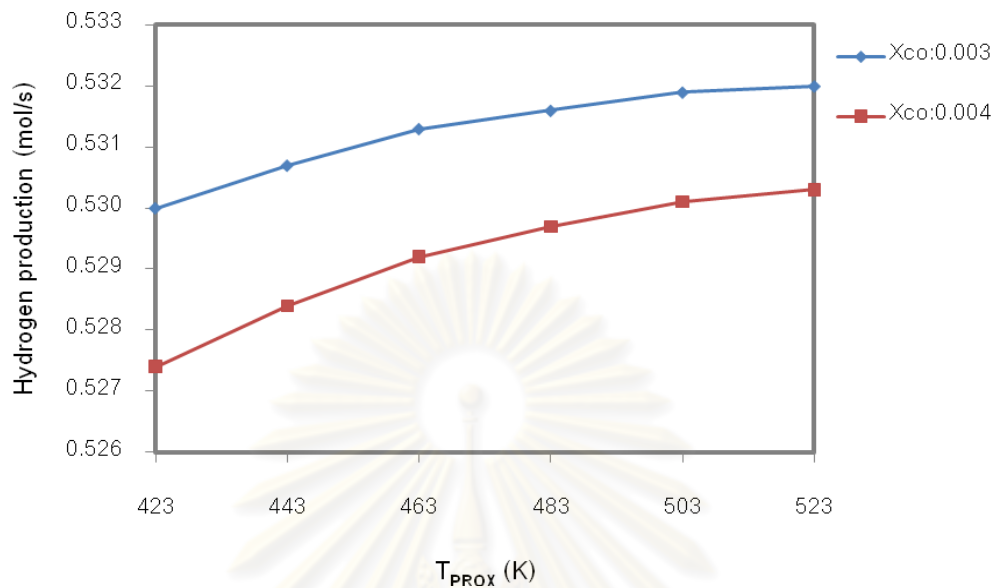


Figure 5.42 Hydrogen production rate of PROX reactor vs. temperature of PROX reactor at the different CO inlet concentrations ($[\text{CO}]_{\text{out}} = 50$ ppm).

Figure 5.42 shows the effect of PROX reactor temperature on hydrogen production rate at CO outlet content of 50 ppm. The results show similar trend as that of SYS I for both levels of CO inlet concentrations. Furthermore, hydrogen loss for case with X_{CO} inlet of 0.003 is less than that with X_{CO} inlet of 0.004. However, at the different CO inlet concentrations can provide hydrogen for PEMFC sufficiently.

Air inlet is fed to PROX reactor to react with reformate for removal CO so, air should be preheated before feeding to the reactor. However, heat required for heat up air inlet should be balanced with the exothermic heat that released from the PROX reactor. The power consumption for the PROX reactor ($Q_4 + Q_5 + Q_6 + Q_{\text{PROX}}$) is shown in Figures 5.43 and 5.44 for the different CO inlet concentrations. More exothermic heat is released for the case with X_{CO} inlet of 0.004 than with X_{CO} inlet of 0.003.

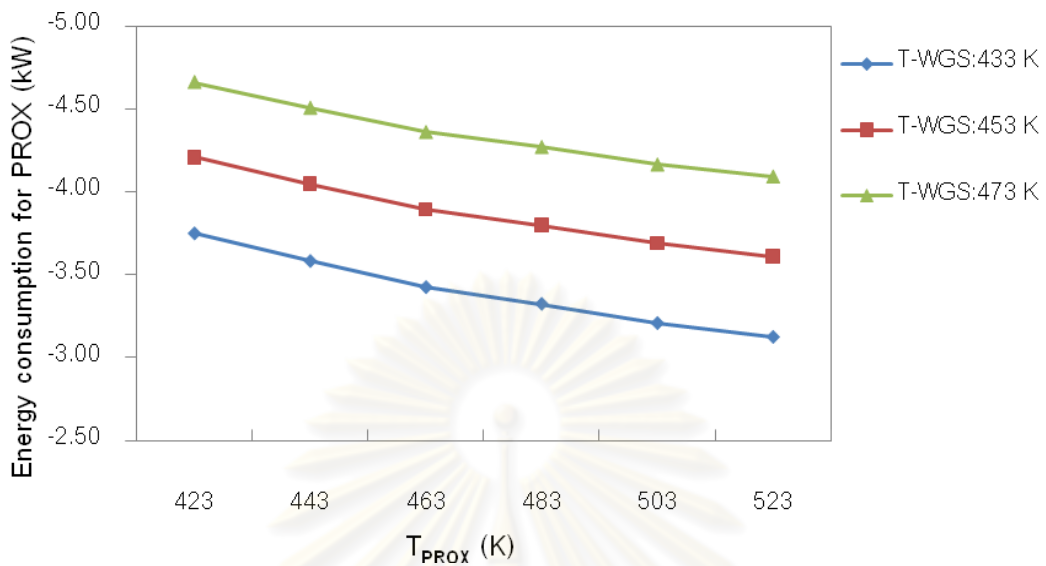


Figure 5.43 Energy consumption for the PROX reactor at X_{CO} inlet of 0.003.

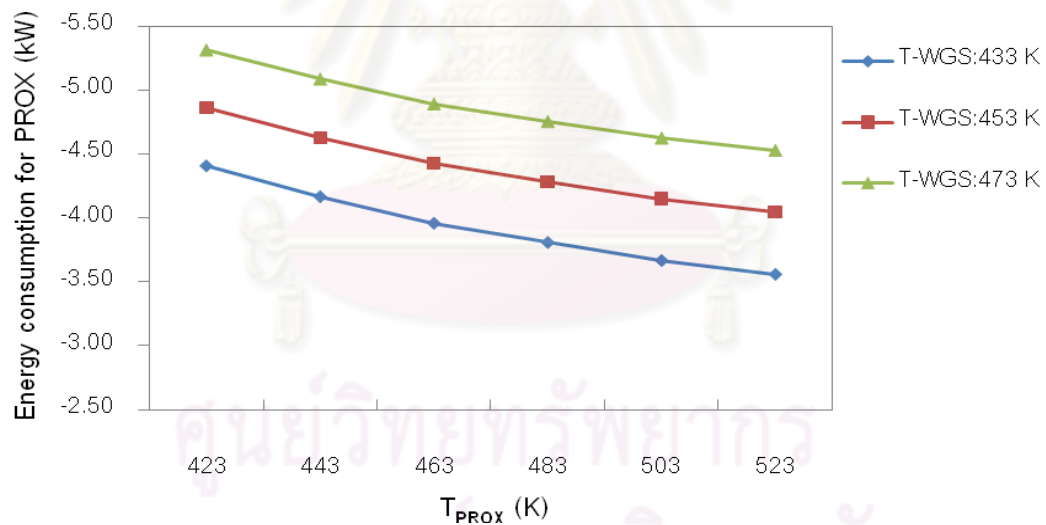


Figure 5.44 Energy consumption for the PROX reactor at X_{CO} inlet of 0.004.

The final hydrogen production rates as Figure 5.42 from SYS II are sufficient to generate the electricity on 50 kW PEMFC at all temperature levels of PROX reactor. So, to select the suitable condition of SYS II, the total catalyst weights and energy consumption of SYS II are investigated. Regarding the results from SYS I, the steam reformer temperature strongly affects total catalyst loading and energy

consumption of systems then, reformer temperature at 533 K is considered for SYS II. Figures 5.45 and 5.46 show the effect of temperature of PROX and WGS reactors on the total catalyst loading for SYS II. At 533 K, temperature of WGS reactor presents the highest total catalyst loading for both of CO inlet contents to PROX reactor and also catalyst loadings at $X_{\text{CO inlet PROX}}$ of 0.003 are higher than that of 0.004 due to contribution of WGS catalyst loading. Therefore, the influence on total catalyst weights is not only from the steam reformer temperature but also from the CO outlet concentration of WGS reactor. For the energy consumption of SYS II at the various PROX and WGS reactor temperatures are shown in Figures 5.47 and 5.48 for $X_{\text{CO inlet PROX}}$ of 0.003 and 0.004, respectively.

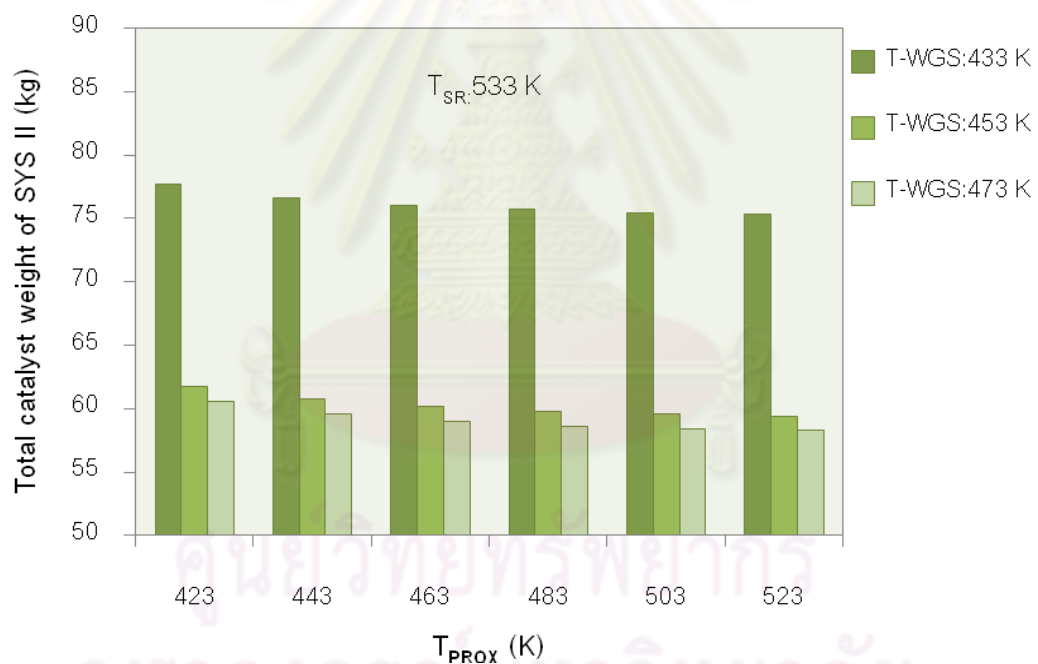


Figure 5.45 Total catalyst weight for SYS II vs. T_{PROX} at the different conditions from the WGS reactor [$X_{\text{CO inlet PROX}} = 0.003$].

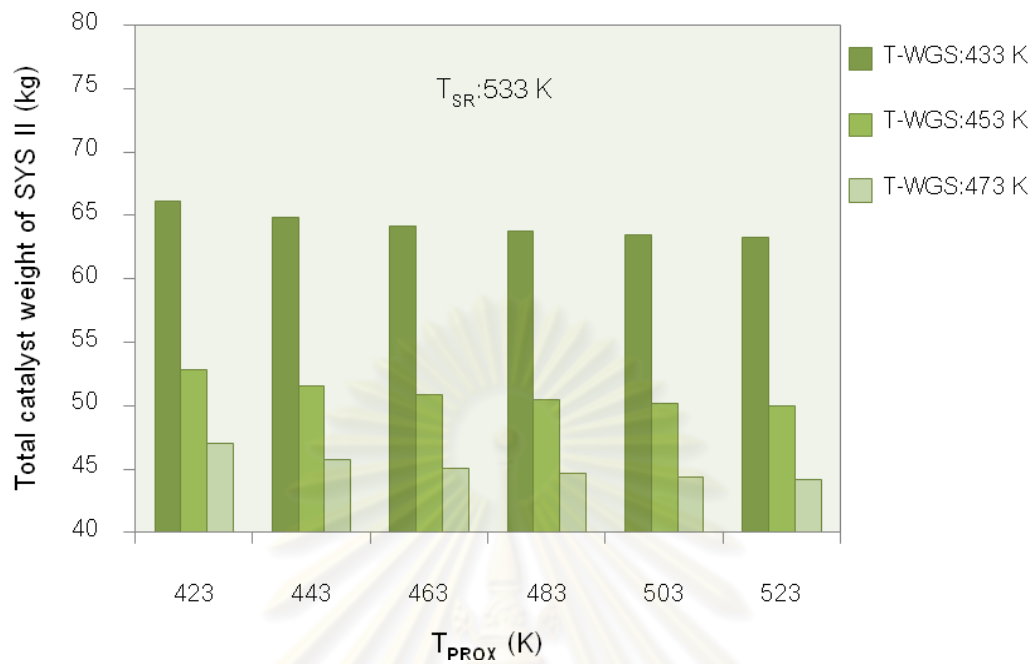


Figure 5.46 Total catalyst weight for SYS II vs. T_{PROX} at different conditions from the WGS reactor [$X_{\text{CO inlet PROX}} = 0.004$].

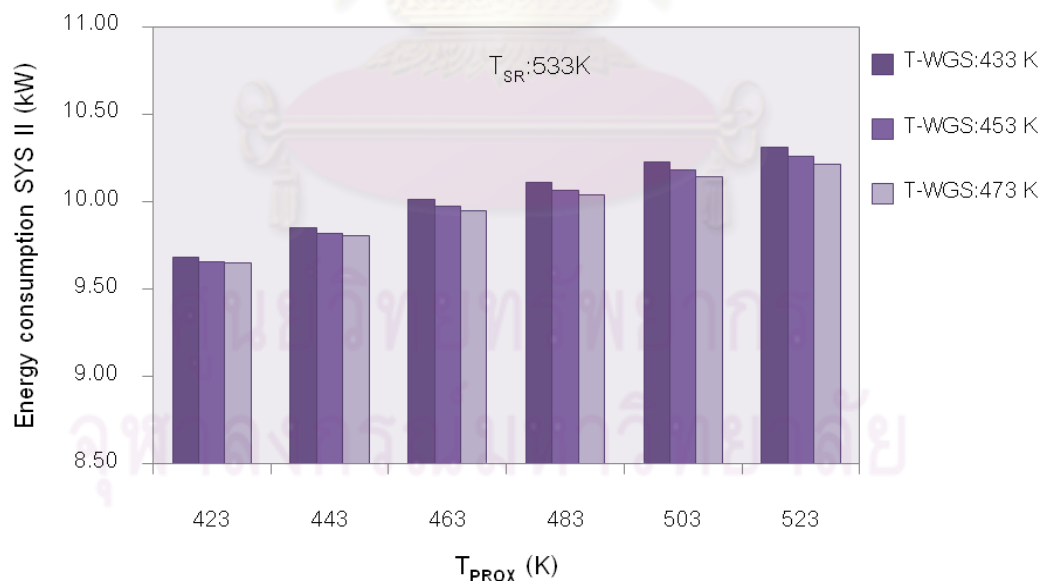


Figure 5.47 Energy consumption for SYS II vs. T_{PROX} at different conditions from the WGS reactor [$X_{\text{CO inlet PROX}} = 0.003$].

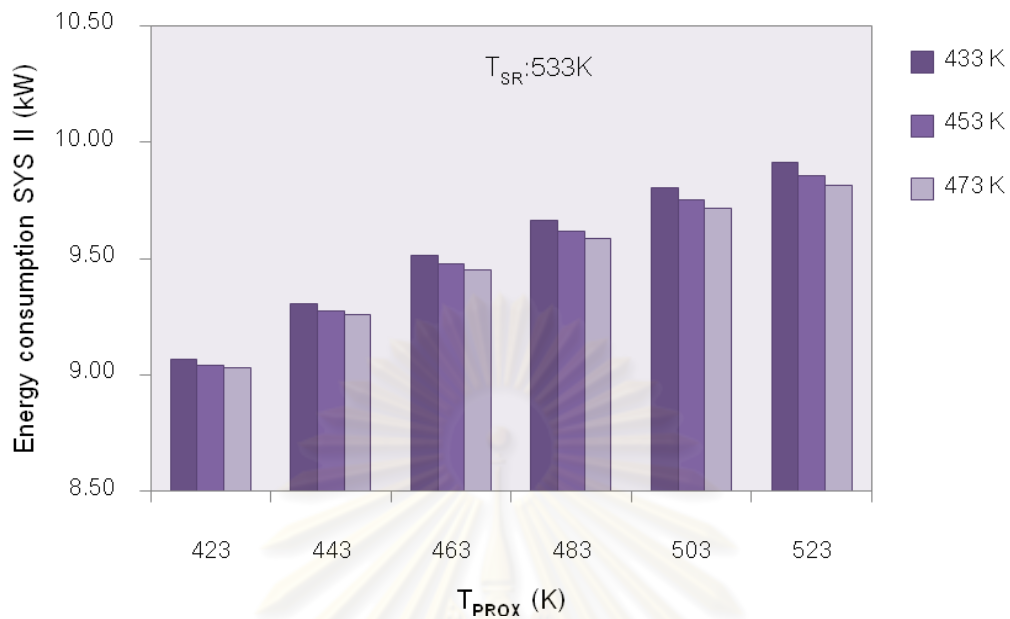


Figure 5.48 Energy consumption for SYS II vs. T_{PROX} at different conditions from the WGS reactor [$X_{\text{CO inlet PROX}} = 0.004$].

Finally, the steam reformer temperature is considered at 533 K and the WGS reactor temperature at 473 K with CO outlet concentration of 0.004. However, the total catalyst weights and energy consumption also depend on PROX reactor temperature because the small catalyst loading occur at higher temperature whereas the energy consumption is very high. So, the selection of a suitable condition for SYS II should consider about the area on the vehicles to make sure that enough for on-board fuel processor and also the heat supply for systems.

5.5 Comparison between SYS I and SYS II

In this study, the on-board fuel processor by methanol are simulated for producing hydrogen enough for 50 kW PEMFC vehicle application. The suitable methanol-fuelled hydrogen production systems are compared between two systems including SYS I (SR and PROX reactor) and SYS II (SR, WGS reactor and PROX reactor).

From the simulation results in the previous section, it was suggested that the suitable steam reformer temperature is 533 K for both SYS I and SYS II because at higher reformer temperature, the catalyst loading significantly decreased as well as total energy consumption. For SYS II, the CO outlet concentration and temperature from WGS reactor influentially affect the volume of reactor. Therefore, as the results from SYS II, the conditions are considered at WGS reactor temperature of 473 K and CO outlet concentration of 0.004. At these conditions for SYS I and SYS II are compared as Figures 5.49, 5.50 and 5.51 in terms of hydrogen production, total catalyst weight and energy consumption, respectively.

SYS I requires lower total catalyst weights than SYS II about 10 kg at each temperature of PROX reactor as shown in Figure 5.50. However the hydrogen production for SYS I is lower than SYS II as shown in Figure 5.49 but it is still sufficient for supplying to PEMFC for vehicle application at 50 kW. The main reason of higher hydrogen production in SYS II is mainly due to the presence of WGS reactor where CO is converted to H₂. The use of WGS reactor in fuel processor promoted the increasing hydrogen production from the further conversion of CO to hydrogen instead of being delivered to PROX reactor. However, hydrogen production rate from SYS II is slightly higher than SYS I of about only 1.3% for this study. For energy consumption as shown in Figure 5.51, both systems show endothermic heat consumption so, external heat is required to supply the systems. However, SYS I demands heat more than SYS II because the exothermic heat from WGS reactor is very high so, the total energy for SYS II is decreased. The temperature of PROX reactor are offered at 523 K because this

condition provides the highest hydrogen production as well as the lowest total catalyst loading, nevertheless, energy consumption is slightly increased.

Finally, a suitable methanol fuel processor is offered to SYS I that composed of steam reformer and preferential oxidation reactor. The reason is mainly from the low total catalyst weight as previously discussed but still sufficiently generate enough hydrogen for PEMFC. The installation of WGS reactor in SYS II, which can reduce the CO concentration to the lowest content only 5×10^{-4} (mole fraction) but the volume of reactor is very high so, it is difficultly equipped in vehicles. While the PROX reactor in SYS I can remove CO in reformat to 50 ppm, the target of this study, with lower catalyst weight when compared with WGS reactor in SYS II. However, SYS I needs heat supply higher than SYS II.

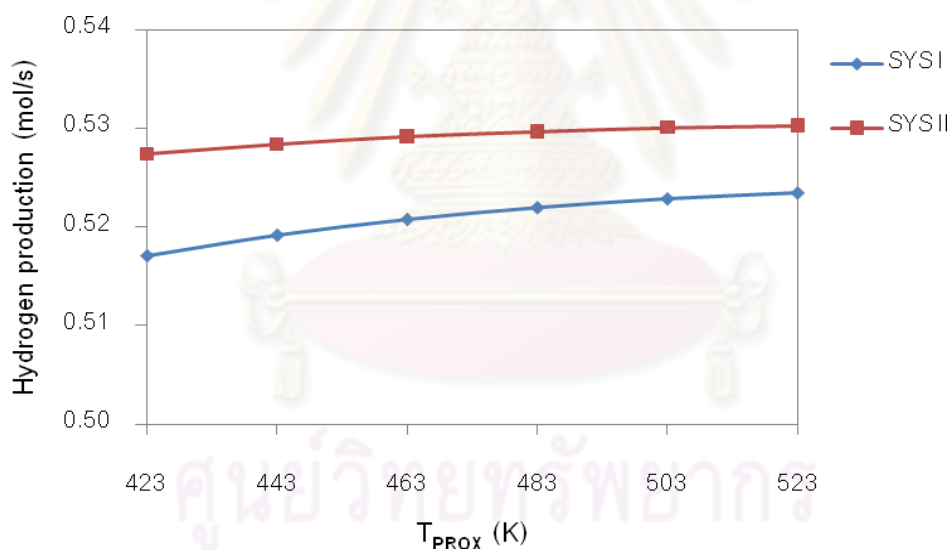


Figure 5.49 The comparison of hydrogen production between SYS I and SYS II.

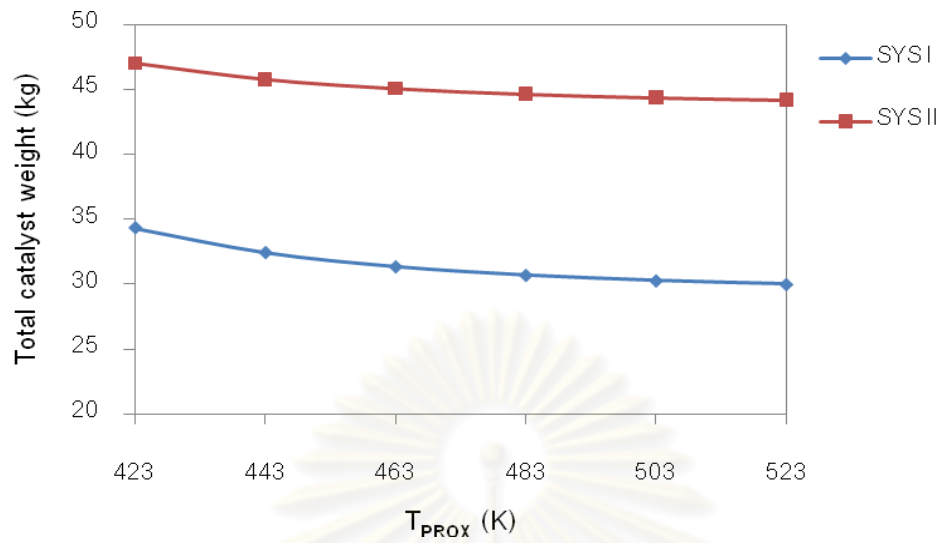


Figure 5.50 The comparison of total catalyst weight between SYS I and SYS II.

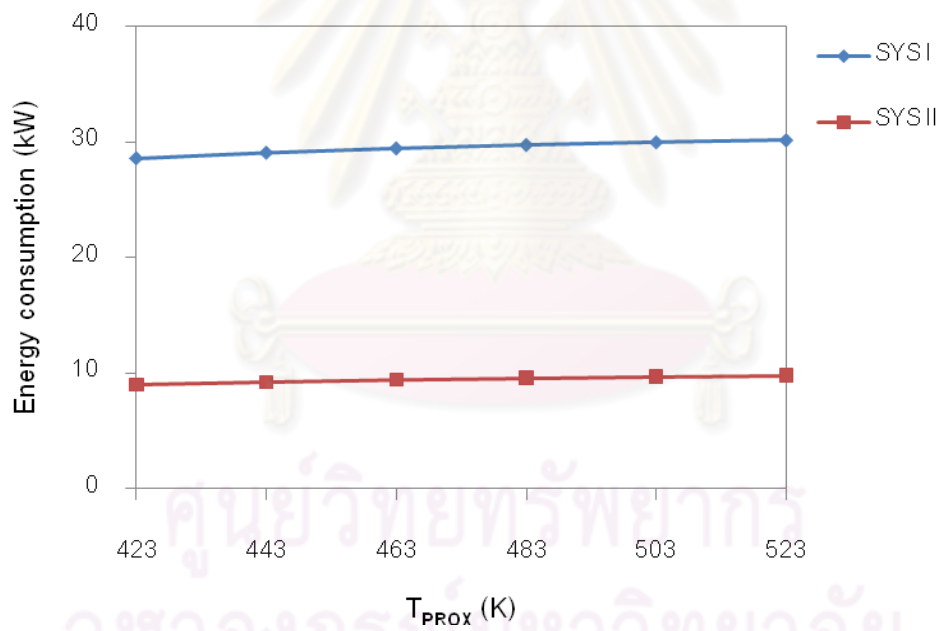


Figure 5.51 The comparison of energy consumption between SYS I and SYS II.

CHAPTER VI

CONCLUSIONS AND RECOMMENDATIONS

6.1 Conclusion

A suitable methanol fuel processor was selected by comparing between SYS I (steam reformer and PROX reactor) and SYS II (steam reformer, WGS reactor and PROX reactor) in terms of hydrogen production, total catalyst weight and energy consumption. The simulations were carried out using MATLAB program. The steam-to-methanol (S/M) molar ratio of 2.0 and 1.5 in the reformer are used in SYS I and SYS II, respectively. The outlet streams from steam reformer are specified at 99.50% MeOH conversion to ensure the sufficient hydrogen and trace amount of unreacted methanol. The oxygen-to-carbon (O/C) molar ratio of 2.0 is simulated for PROX reactor for both of systems and the target of CO concentration is set at 50 ppm. For SYS II, the reformat at 99.50% MeOH conversion from the steam reformer are fed to the WGS reactor. Additional amount of water is fed to the WGS reactor which make the over S/M ratio equivalent for both SYS I and SYS II.

The performance of SYS I and SYS II are investigated in terms of total catalyst weight, hydrogen production and energy consumption at various temperatures of steam reformer, WGS reactor (only for SYS II) and PROX reactor. The simulation results indicate that the increasing temperatures of SR and PROX result in significant reduction of catalyst weight for each of reactor. Hydrogen production is decreased by the rising temperature of SR but the opposite trend is observed in the PROX. The WGS reactor is purposed to reduce CO in SR outlet streams, moreover, the hydrogen production rate is promoted but it is not quite significant as observed in this study. The CO conversion for WGS reactor is controlled by the equilibrium conversion so, the increasing temperature is not favorable in term of CO reduction. The key parameter of WGS reactor is the CO outlet concentration if it offered very low that means the volume of WGS reactor is very large. For energy consumption, the reactions occurred in steam reformer are endothermic reaction but in contrast, WGS and PROX reactors involve

exothermic reactions especially, the WGS reactor which is quite highly exothermic. For this reason, SYS II required external heat to supply the system lower than SYS I.

In conclusion, SYS I is considered as a suitable system to produce hydrogen for PEMFC 50 kW with 29.20 and 0.80 kg for the volume of steam reformer and PROX reactor, respectively.

6.2 Recommendation

The design of systems based on non-isothermal and two-dimensional models is recommended for future work and also the combination of this system with PEMFC should be considered. Some heat can be released to provide for steam reformer by PEMFC. This recommendation can help clearly understand more on the real systems. In addition, the type of catalyst should be considered because the new type may present higher activity or selectivity so that will be applied to increase the performance of fuel processor.



ศูนย์วิทยทรัพยากร
จุฬาลงกรณ์มหาวิทยาลัย

REFERENCES

- Ahmed, S. and Krumpelt, M., Hydrogen from hydrocarbon fuels for fuel cells. International Journal of Hydrogen Energy 26 (2001): 291-301.
- Amphlett, J. C., et al., Hydrogen production by steam reforming of methanol for polymer electrolyte fuel cells. International Journal of Hydrogen Energy 19 (1994): 131-137.
- Avci, A. K., Önsan, Z. I. and Trimm, D. L., On-board fuel conversion for hydrogen fuel cells: Comparison of different fuels by computer simulations. Applied Catalysis A: General 216 (2001): 243-256.
- Brown, L. F., A comparative study of fuels for on-board hydrogen production for fuel-cell-powered automobiles. International Journal of Hydrogen Energy 26 (2001): 381-397.
- Choi, Y. and Stenger, H. G., Kinetics, simulation and insights for co selective oxidation in fuel cell application. Journal of Power Sources 129 (2004): 246-254.
- Choi, Y. and Stenger, H. G., Kinetics, simulation and optimization of methanol steam reformer for fuel cell applications. Journal of Power Sources 142 (2005): 81-91.
- Choi, Y. and Stenger, H. G., Water gas shift reaction kinetics and reactor modeling for fuel cell grade hydrogen. Journal of Power Sources 124 (2003): 432-439.
- Dudfield, C. D., Chen, R. and Adcock, P. L., A carbon monoxide prox reactor for PEM fuel cell automotive application. International Journal of Hydrogen Energy 26 (2001): 763-775.
- Ersoz, A., Olgun, H. and Ozdogan, S., Reforming options for hydrogen production from fossil fuels for PEM fuel cells. Journal of Power Sources 154 (2006): 67-73.

- Francesconi, J. A., Mussati, M. C. and Aguirre, P. A., Analysis of design variables for water-gas-shift reactors by model-based optimization. Journal of Power Sources 173 (2007): 467-477.
- Francesconi, J. A., Mussati, M. C., Mato, R. O. and Aguirre, P. A., Analysis of the energy efficiency of an integrated ethanol processor for PEM fuel cell systems. Journal of Power Sources 167 (2007): 151–161.
- Gallucci, F., Paturzo, L. and Basile, A., Hydrogen recovery from methanol steam reforming in a dense membrane reactor: Simulation study. Ind. Eng. Chem. Res. 43 (2004): 2420-2432.
- Kamarudin, S. K., et al., The conceptual design of a PEMFC system via simulation. Chemical Engineering Journal 103 (2004): 99–113.
- Kamarudin, S. K., et al., Design of a fuel processor unit for PEM fuel cell via shortcut design method. Chemical Engineering Journal 104 (2004): 7-17.
- Kolavennu, P. K., Telotte, J. C. and Palanki, S., Design of a fuel cell power system for automotive applications. International Journal of Chemical Reactor Engineering 4 (2006): 1-15.
- Lattner, J. R. and Harold, M. P., Comparison of conventional and membrane reactor fuel processors for hydrocarbon-based PEM fuel cell systems. International Journal of Hydrogen Energy 29 (2004): 393-417.
- Lattner, J. R. and Harold, M. P., Comparison of methanol-based fuel processors for PEM fuel cell systems. Applied Catalysis B:Environmental 56 (2005): 149-169.
- Lindstrom, B. and Pettersson, L. J., Hydrogen generation by steam reforming of methanol over copper-based catalysts for fuel cell applications. International Journal of Hydrogen Energy 26 (2001): 923-933.

- Lwin, Y., Daud, W. R. I. W., Mohamad, A. B. and Yaakob, Z., Hydrogen production from steam-methanol reforming: Thermodynamic analysis. International Journal of Hydrogen Energy 25 (2000): 47-53.
- Oliva, D. G., Francesconi, J. A., Mussati, M. C. and Aguirre, P. A., Co-PrOx reactor design by model-based optimization. Journal of Power Sources 182 (2008): 307-316.
- Ouzounidou, M., Ipsakis, D., Voutetakis, S., Papadopoulou, S. and Seferlis, P., A combined methanol autothermal steam reforming and PEM fuel cell pilot plant unit: Experimental and simulation studies. Energy 34 (2009): 1733-1743.
- Peppley, B. A., Amphlett, J. C., Kearns, L. M. and Mann, R. F., Methanol-steam reforming on Cu/ZnO/Al₂O₃ catalysts. Part 2. A comprehensive kinetic model. Applied Catalysis A: General 179 (1999): 31-49.
- Rabenstein, G. and Hacker, V., Hydrogen for fuel cells from ethanol by steam-reforming, partial-oxidation and combined auto-thermal reforming: A thermodynamic analysis. Journal of Power Sources 185 (2008): 1293-1304.
- Ratnamala, G. M., Shah, N., Mehta, V., Rao, P. V. and Devotta, S., Integrated fuel cell processor for a 5-kw proton-exchange membrane fuel cell. Ind. Eng. Chem. Res. 44 (2005): 1535-1541.
- Schumacher, N., et al., Trends in low-temperature water-gas shift reactivity on transition metals. Journal of Catalysis 229 (2005): 265-275.
- Telotte, J. C., Kern, J. and Palanki, S., Miniaturized methanol reformer for fuel cell powered mobile applications. International Journal of Chemical Reactor Engineering 6 (2008): 1-15.
- Vahabi, M. and Akbari, M. H., Three-dimensional simulation and optimization of an isothermal PROX microreactor for fuel cell applications. International Journal of Hydrogen Energy 34 (2009): 1531-1534.



APPENDICES

ศูนย์วิทยทรัพยากร
จุฬาลงกรณ์มหาวิทยาลัย

APPENDIX A

THE MATRIX OF ODINARY EQUATIONS

From the mole balances of steam reformer, water-gas shift reactor and preferential oxidation reactor, we can write these equations in matrix below. For all reactors the molar balances of components can be calculated from equations (A.1)-(A.14).

1. Steam reformer

The molar balance for the steam reformer, we can provide as below:

For the species;

$$\frac{dF_{CH_3OH}}{dW} = [-r_R - r_D] \quad (A.1)$$

$$\frac{dF_{H_2O}}{dW} = [-r_R - r_W] \quad (A.2)$$

$$\frac{dF_{CO}}{dW} = [r_D - r_W] \quad (A.3)$$

$$\frac{dF_{CO_2}}{dW} = [r_R + r_W] \quad (A.4)$$

$$\frac{dF_{H_2}}{dW} = [3r_R + 2r_D + r_W] \quad (A.5)$$

2. Water-gas shift reactor

The molar balance for the water-gas shift reactor, we can provide as below:

For the species;

$$\frac{dF_{CO}}{dW} = [-r_{WGS}] \quad (\text{A.6})$$

$$\frac{dF_{H_2O}}{dW} = [-r_{WGS}] \quad (\text{A.7})$$

$$\frac{dF_{CO_2}}{dW} = [r_{WGS}] \quad (\text{A.8})$$

$$\frac{dF_{H_2}}{dW} = [r_{WGS}] \quad (\text{A.9})$$

3. Preferential oxidation reactor

The molar balance for the preferential oxidation reactor, we can provide as below:

For the species;

$$\frac{dF_{CO}}{dW} = [-r_{CO} - r_{WGS,P}] \quad (\text{A.10})$$

$$\frac{dF_{O_2}}{dW} = [-0.5r_{CO} - 0.5r_{H_2}] \quad (\text{A.11})$$

$$\frac{dF_{H_2O}}{dW} = [r_{H_2} - r_{WGS,P}] \quad (\text{A.12})$$

$$\frac{dF_{CO_2}}{dW} = [r_{CO} + r_{WGS,P}] \quad (\text{A.13})$$

$$\frac{dF_{H_2}}{dW} = [-r_{H_2} + r_{WGS,P}] \quad (\text{A.14})$$

APPENDIX B

THE PROPERTIES OF COMPONENTS

The components of all reactors in this work are methanol (CH₃OH), steam (H₂O), oxygen (O₂), carbon monoxide (CO), carbon dioxide (CO₂), hydrogen (H₂) and nitrogen (N₂). The Gibbs free energy of formation of these components in relation $G_f = A + BT + CT^2$ is shown in Table B.1. In addition, the heat capacity in relation $C_p = a + bT + cT^2 + dT^3 + eT^4$ and the heat of formation in relation $H_f = A + BT + CT^2$ are presented in Table B.2 and B.3, respectively.

Table B.1 Gibb's free energy of formation (G_f) of components (kJ/mol).

Components	$G_f = A + BT + CT^2$ [kJ/mol]		
	a	$b \times 10^2$	$c \times 10^6$
CH ₃ OH	-201.86	12.542	20.345
H ₂ O	-241.74	4.174	7.4281
CO	-109.885	-9.2218	1.4547
CO ₂	-393.36	-0.38212	1.3322
H ₂	0	0	0
O ₂	0	0	0
N ₂	0	0	0

Table B.2 Heat capacities (C_p) of components (J/mol).

Components	$C_p = a + bT + cT^2 + dT^3 + eT^4$ [J/mol]				
	a	$b \times 10^3$	$c \times 10^5$	$d \times 10^8$	$e \times 10^{13}$
Methanol (g)	40.046	-38.287	24.529	-21.679	599.09
Methanol (l)	40.152	310.46	-102.91	145.98	0
Water (g)	33.933	-8.4186	2.9906	-1.7825	36.934
Water (l)	92.053	-39.953	-21.103	53.469	0
Carbon monoxide	29.556	-6.5807	2.013	-1.2227	22.617
Carbon dioxide	27.437	42.315	-1.9555	0.3997	-2.9872
Hydrogen	25.399	20.178	-3.8549	3.188	-87.585
Oxygen	29.526	-8.8999	3.8083	-3.2629	88.607
Nitrogen	29.342	-3.5395	1.0076	-0.43116	2.5935

Table B.3 Heat of formation (H_f) of components (kJ/mol)

Components	$H_f = A + BT + CT^2$ [kJ/mol]		
	a	$b \times 10^3$	$c \times 10^5$
Methanol (g)	-188.188	-49.823	2.0791
Water (g)	-238.41	-12.256	27.656
CO	-112.19	8.1182	-8.0425
CO ₂	-393.422	0.1591	-0.1395
H ₂	0	0	0
O ₂	0	0	0
N ₂	0	0	0

APPENDIX C

LIST OF PUBLICATION

Siriporn Boonkrue, Worapon Kiatkittipong, Amornchai Arpornwichanop, Navadol Laosiripojana, Apinan Soottitantawat, Wisitsree Wiyaratn and Suttichai Assabumrungrat, "Design of hydrogen production system for application in polymer electrolyte membrane fuel cell vehicle", Pure and Applied Chemistry International Conference 2010, Ubon Ratchathani, Thailand, January, 2010, (poster presentation).



ศูนย์วิทยทรัพยากร
จุฬาลงกรณ์มหาวิทยาลัย

VITA

Miss Siriporn Boonkrue was born in Chumporn, Thailand on December 01, 1983. She received Bachelor's degree of Engineering from the department of Chemical Engineering, Faculty of Engineering, Prince of Songkla University, Songkhla, Thailand in 2006 and completed Master's degree of Engineering from the department of Chemical Engineering, Faculty of Engineering, Chulalongkorn University, Bangkok, Thailand in 2010.



ศูนย์วิทยทรัพยากร
จุฬาลงกรณ์มหาวิทยาลัย